Calorimetry

Riccardo Paramatti

Cern & INFN Roma

IPMLHC2013

Tehran – 9th October

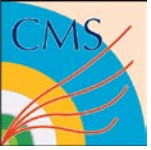

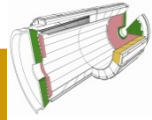

Outline

The talk is an introduction to calorimetry with focus on the CMS electromagnetic and hadronic calorimeters

- Particle interaction with matter
- Electromagnetic and hadronic showers
- Detection mechanisms
- Homogeneous and sampling calorimeters
- Energy resolution
- Compensation & Energy Flow

Suggested reading: Calorimetry by Richard Wigmans
Many plots taken from his talks.

- The CMS calorimeters
- Few examples about performance of CMS calorimeters

Calorimeters: a simple concept

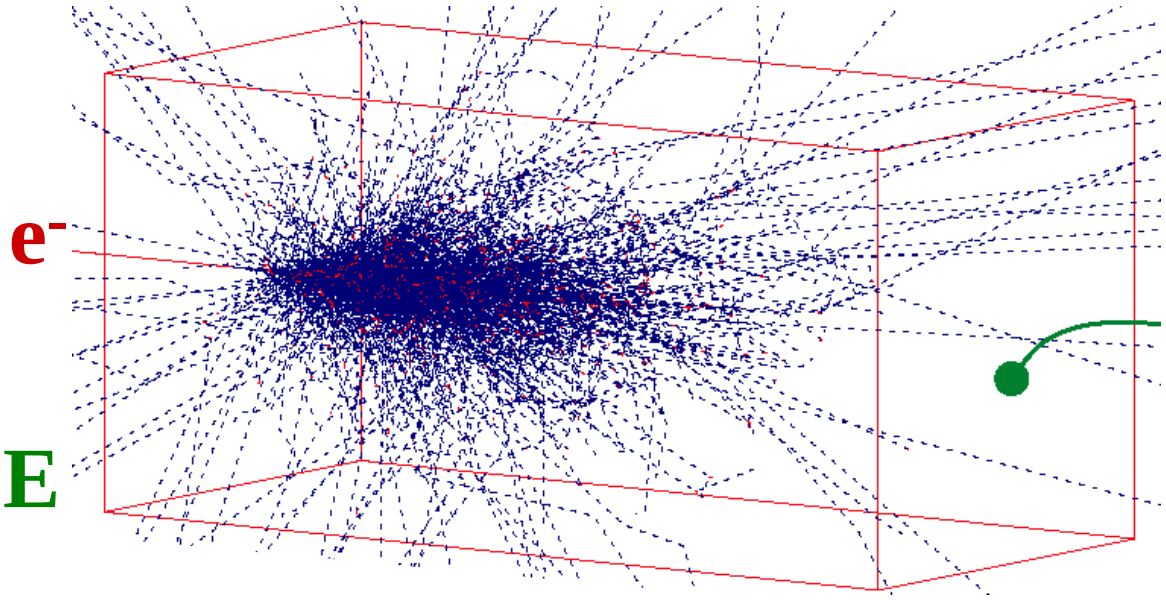

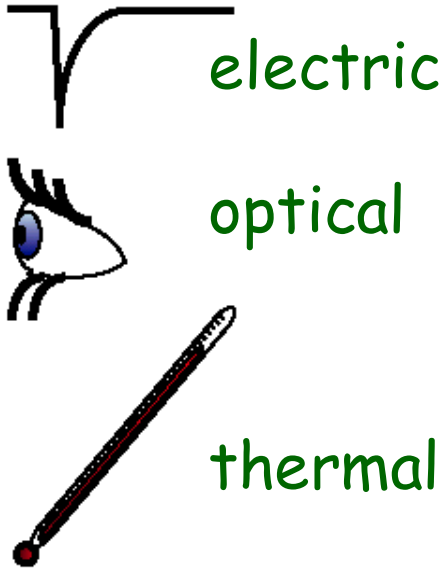

Convert energy **E** of incident particle to detector response **S**: $S \propto E$

The temperature effect of a 100 GeV particle in 1 litre of water (at 20 °C) is: $\Delta T = 3.8 \cdot 10^{-12}\, K$

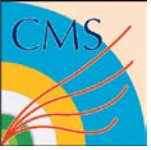

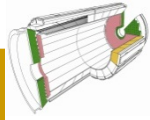

Calorimeters: some features

- Detection of both charged and neutral particles
- Particle identification by simple topological algorithms
- Detection based on stochastic processes
  - precision increases with E
- Dimensions necessary to containment ∝ lnE
  - compactness
- Segmentation
  - measure of position and direction
- Fast
  - high rate capability, trigger

Calorimetry is a "destructive" method. Energy and particle get absorbed !

Particles in CMS detector

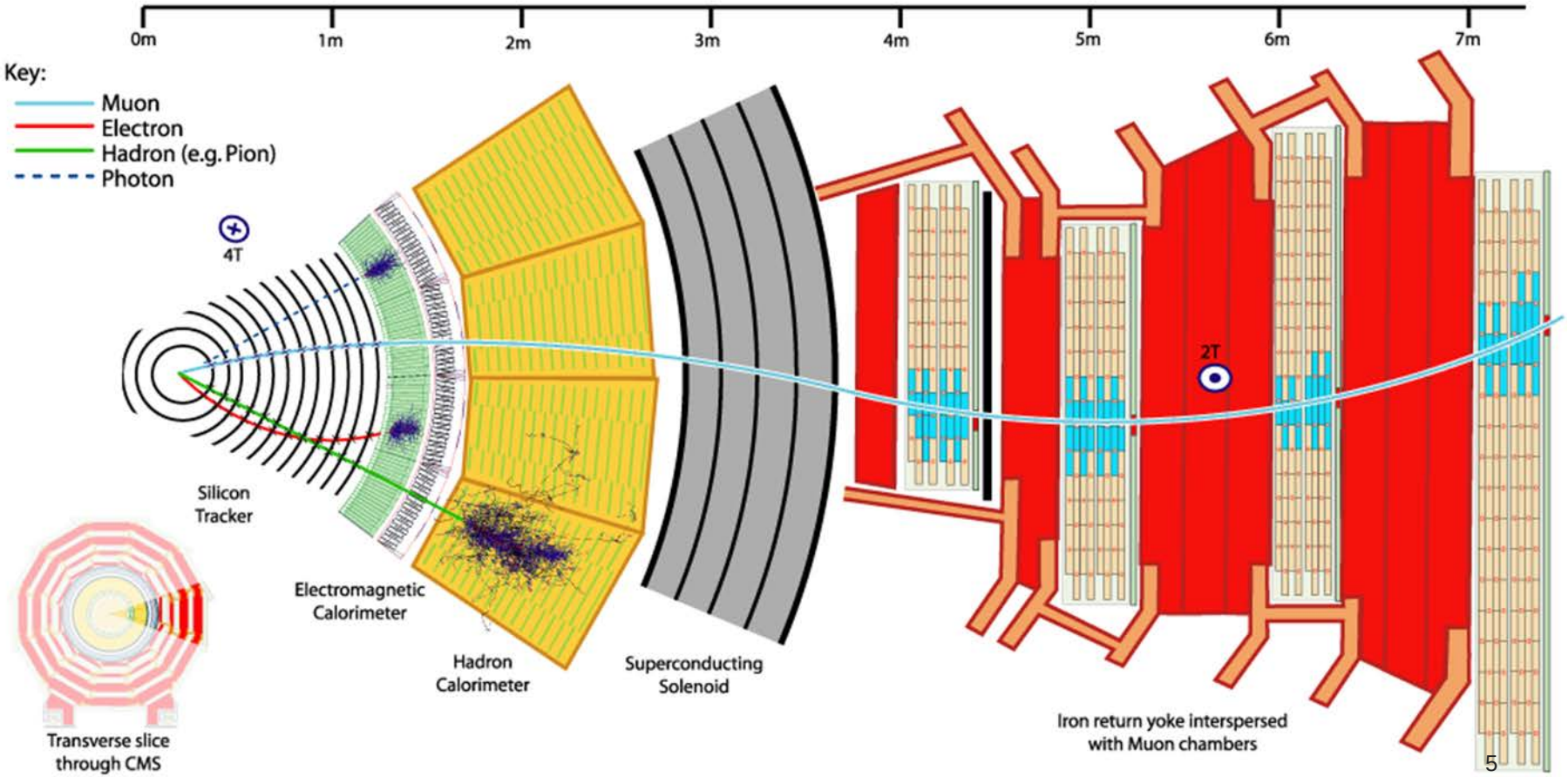

Resolution: calorimeter vs tracker

tracker momentum measurement with the sagitta method

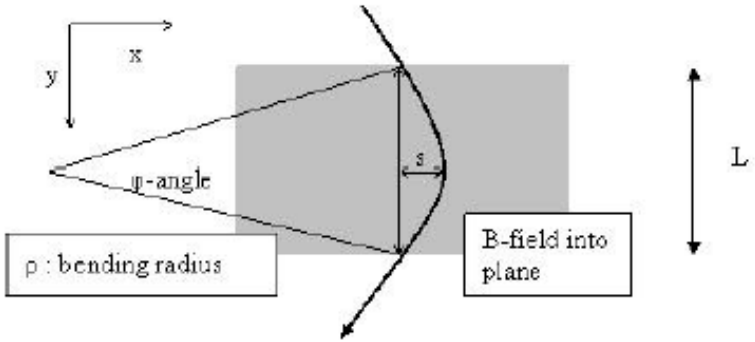

$$\frac{\sigma(p_T)}{p_T} = \frac{\sigma(x)\, p_T}{0.3BL^2}\sqrt{720/(N+4)}$$

In CMS the contribution to the electron energy measurement from the tracker is relevant below ~20 GeV.

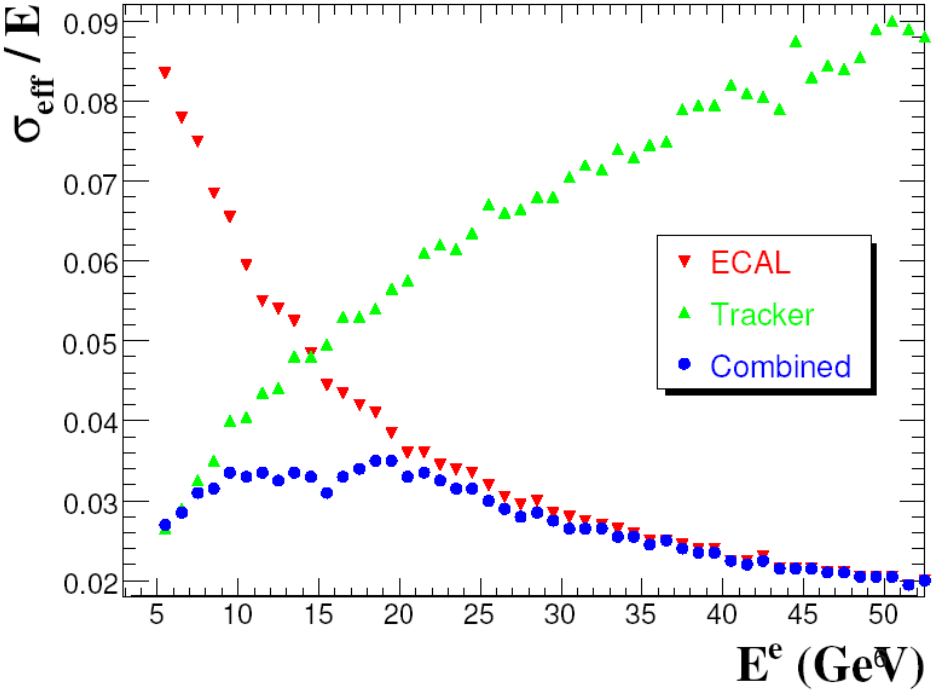

Energy loss – electrons (1)

- Ionization : mean energy loss given by Bethe-Bloch

$$\left\langle \frac{dE}{dx} \right\rangle = -4\pi N_A r_e^2 m_e c^2 z^2 \frac{Z}{A}\frac{1}{\beta^2}\left[\frac{1}{2}\ln\frac{2m_e c^2\gamma^2\beta^2 T^{\max}}{I^2} - \beta^2 - \frac{\delta}{2}\right]$$

$\sigma \propto Z$

$\sigma \propto \ln E/m_e$

Electrons require some corrections due to their small mass and Pauli principle.

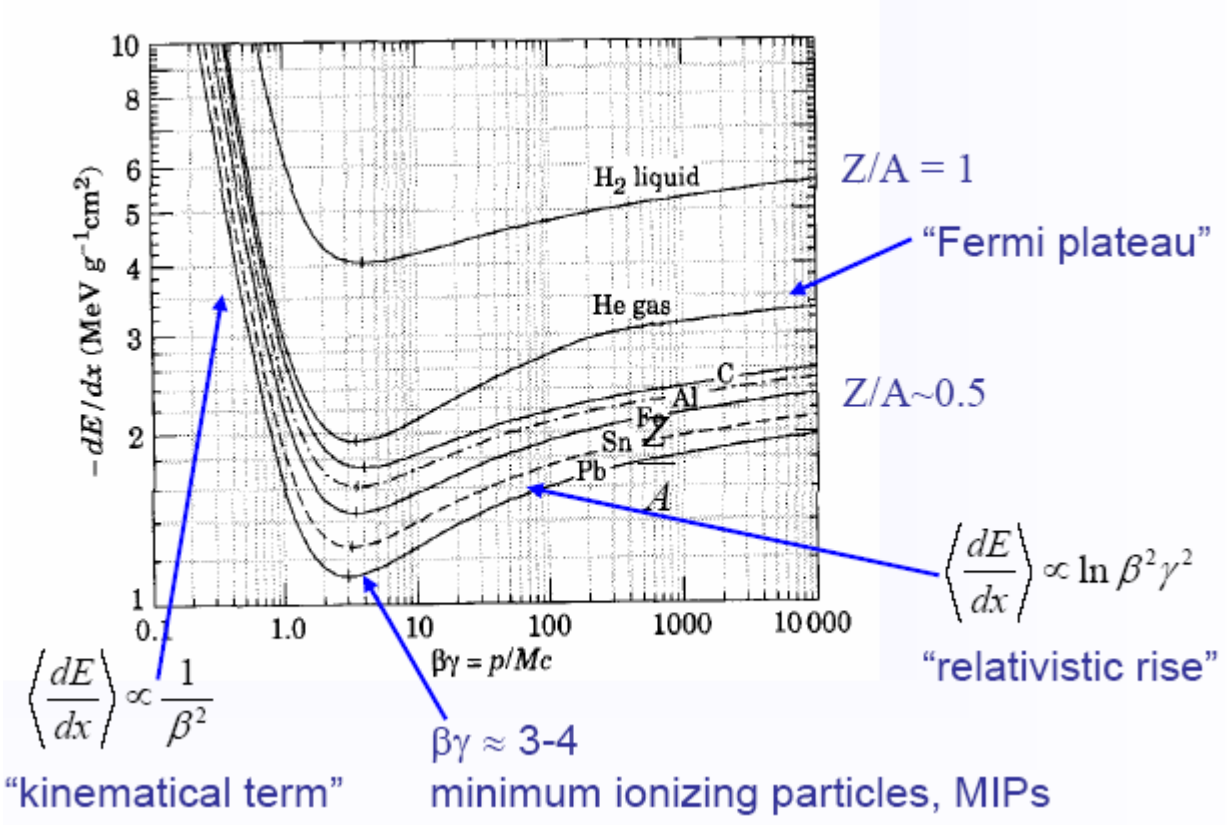

Energy loss – electrons (2)

- bremsstrahlung

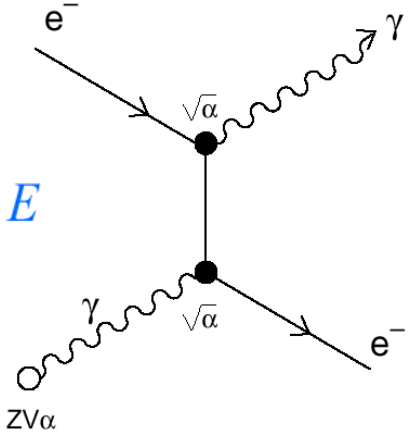

➢ energy loss $$-\frac{dE}{dx}\Big|_{rad} = \left[4n\,\frac{Z^2\alpha^3(\hbar c)^2}{m_e^2c^4}\,\ln\frac{183}{Z^{1/3}}\right]E$$

$$-\frac{dE}{dx} \propto \frac{Z^2E}{m^2} \qquad \langle\Theta\rangle = \frac{1}{\gamma}$$

$$X_0 = \left[4n\,\frac{Z^2\alpha^3(\hbar c)^2}{m_e^2c^4}\,\ln\frac{183}{Z^{1/3}}\right]^{-1}$$

Radiation length: thickness of material that reduces the mean energy of a beam of high energy electrons by a factor e

$$\frac{dE}{dx} = -\frac{E}{X_0} \quad and \quad X_0 \approx \frac{180A}{Z^2}\ g.cm^{-2}$$

in air: 300 m
in plastic scintillator: 40 cm
in iron: 1.76 cm

$\sigma \propto Z(Z+1)$; $\propto \ln E/m_e$ for $E < 1$ GeV independent of energy above

Energy loss – electrons (3)

- **Critical energy E_c:**

$$\frac{(dE/dx)_{rad}}{(dE/dx)_{ion}} = 1$$

$$E_c \approx \frac{610\text{MeV}}{Z + 1.24}$$

(solids, liquids)

Strongly material dependent, it scales as 1/Z
(eg. 7 MeV for lead, 20 MeV for copper; 1 TeV for muons in copper !)

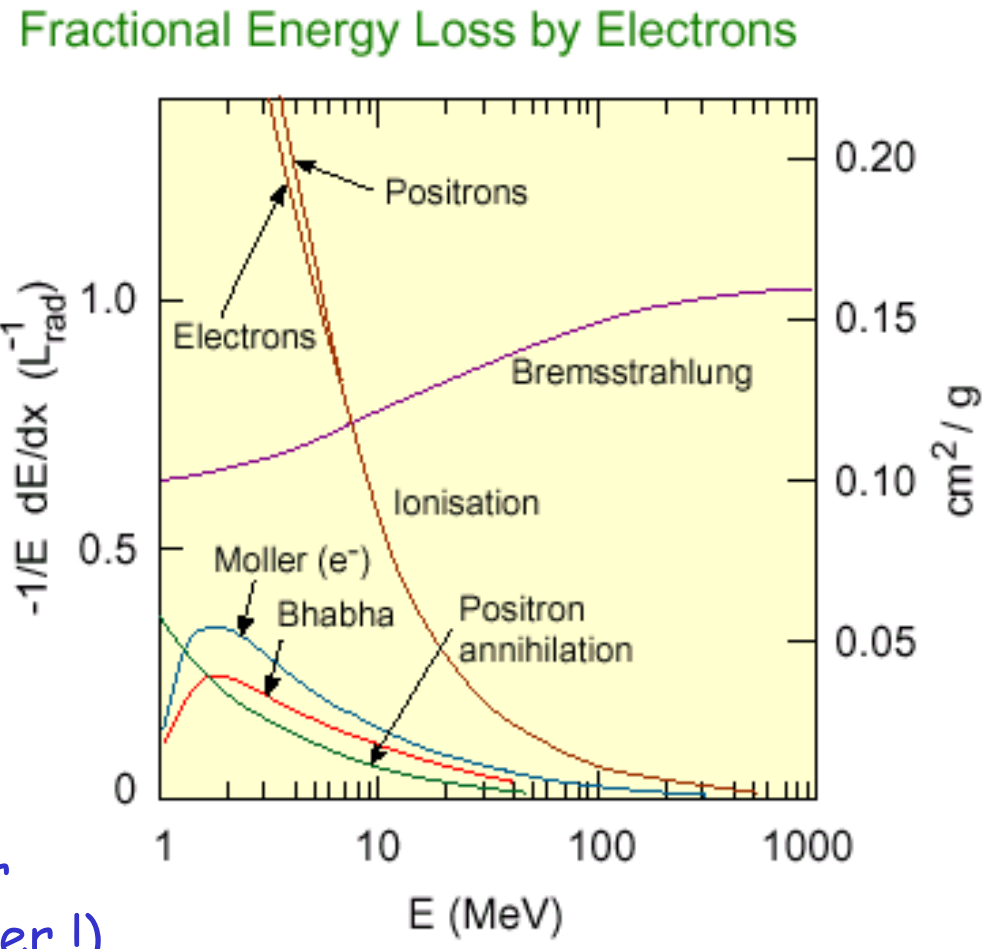

Energy loss – photons (1)

- photo-electric effect

$$\sigma_{pe} \approx Z^5 \alpha^4 \left(\frac{m_e c^2}{E_\gamma} \right)^{\frac{7}{2}} \qquad \sigma \propto Z^5 \ , \ E^{-3.5}$$

- compton scattering

$$\sigma_c \approx Z \frac{\ln E_\gamma}{E_\gamma} \qquad \sigma \propto Z \ , \ E^{-1}$$

- pair production occours if $E_\gamma > 2m_e c^2$

$$\sigma_{pair} \approx \frac{7}{9} \frac{A}{N_A} \frac{1}{X_0}$$

- $\sigma \propto Z\,(Z+1)$; $\propto \ln E/m_e$ for $E < 1\,GeV$ independent of energy above 1 GeV
- Probability of conversion in $1X_0$ is $e^{-7/9}$
- Mean free path $L_{pair} = 9/7\ X_0$ (γ disappears)

Energy loss – photons (2)

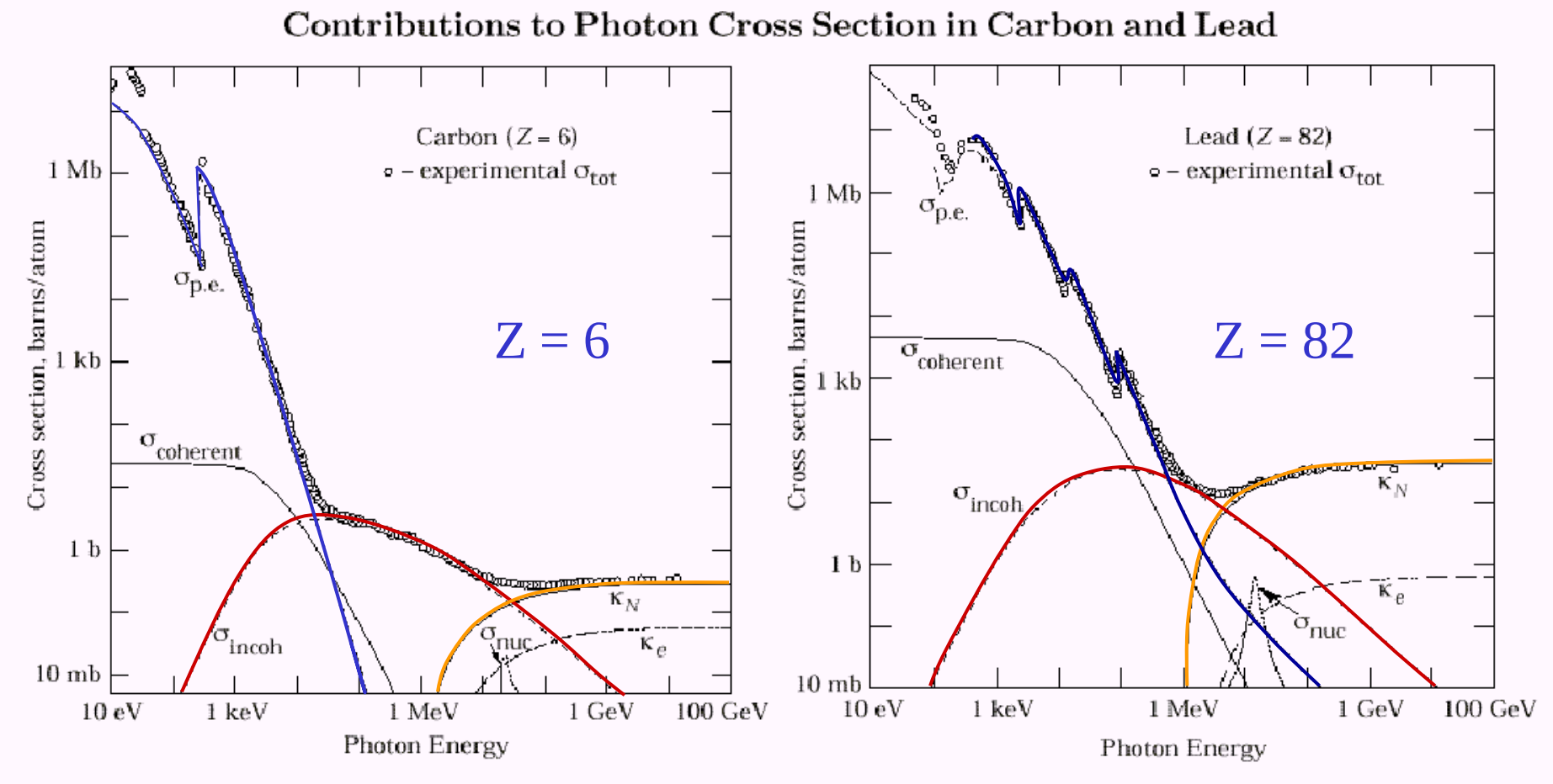

Cross section in right plot: more lead is needed to absorbe a photon with 20 MeV energy than a 3 MeV photon !!

Energy loss – photons (3)

Main contribution to cross section

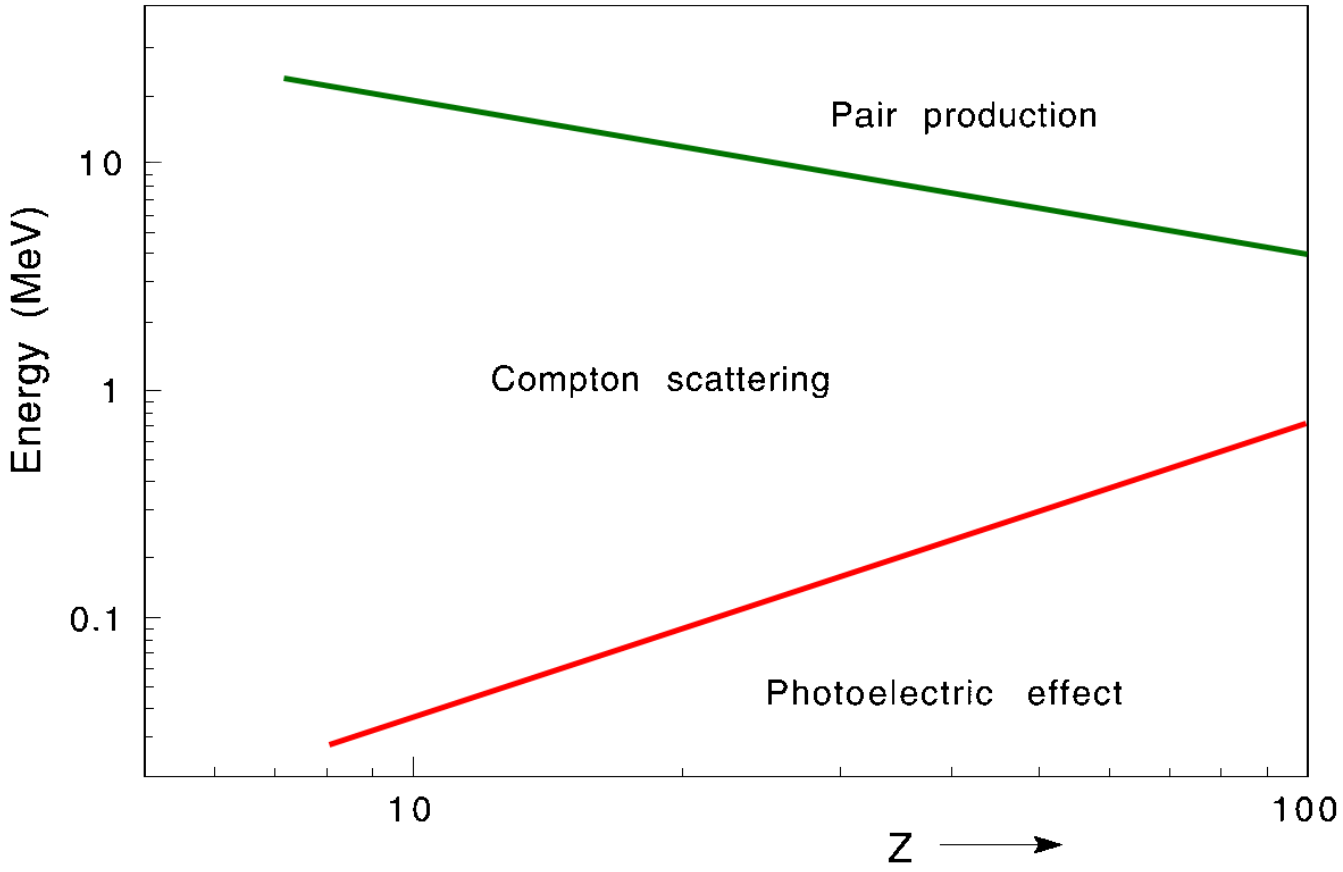

Electromagnetic Shower

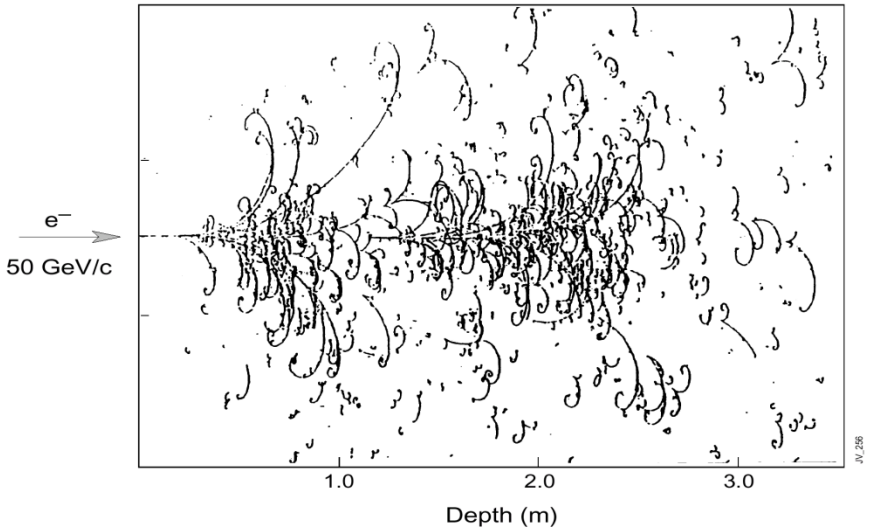

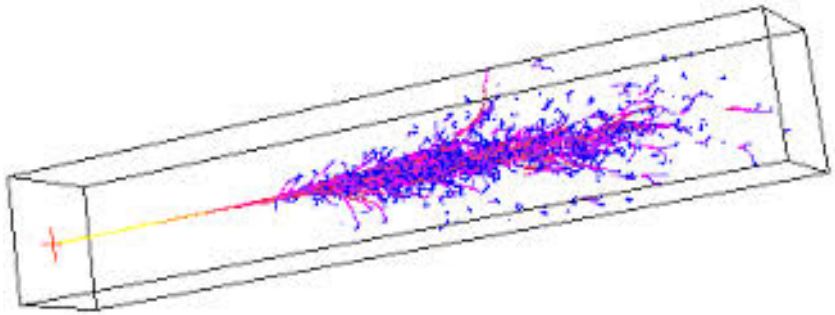

Big European Bubble Chamber filled with Ne:H_2 = 70%:30%,
3T Field, L=3.5 m, X_0≈34 cm, 50 GeV incident electron

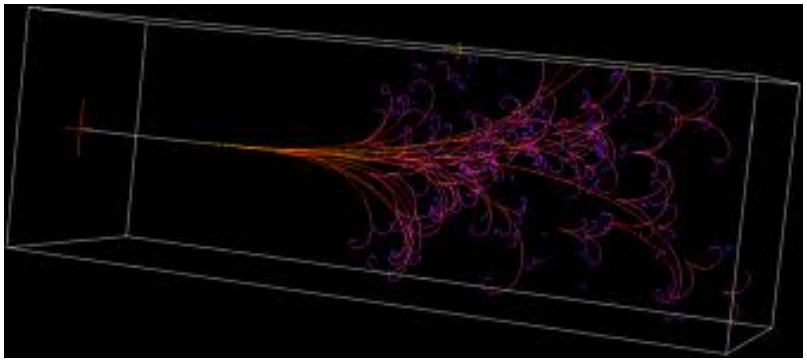

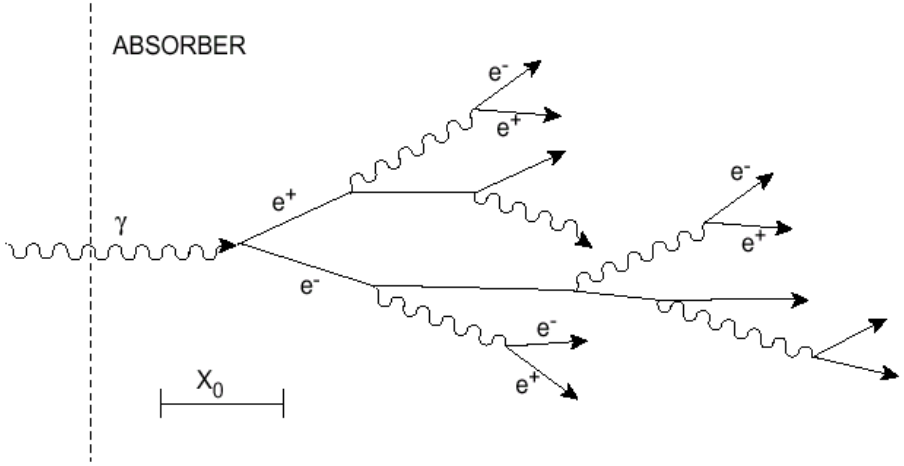

Electromagnetic Shower (2)

Above 1 GeV the dominant processes, bremsstrahlung for e^+ and e^- and pair production for γ, become energy independent

Trough a succession of these energy loss mechanisms an electromagnetic cascade is propagated until the energy of charged secondaries has been degraded to the regime dominated by ionization loss (below E_c)

Below E_c a slow decrease in number of particles occurs as electrons are stopped and photons absorbed

Electromagnetic Shower (3)

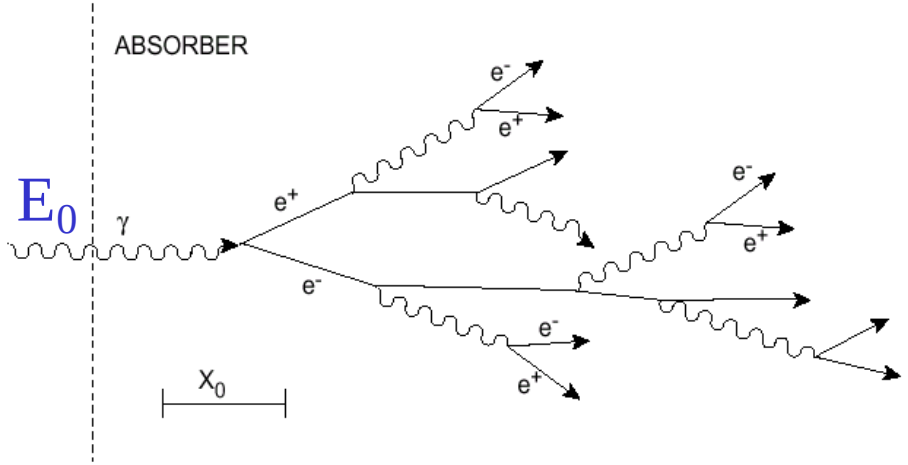

- In $1X_0$ an e loses about 2/3 of its E a high energy γ has a probability of 7/9 of pair conversion
- Assume X_0 as a generation length
- In each generation the number of particle increases by a factor 2

@$\Delta x=X_0$ $\gamma \rightarrow$ e+ e- $E=E_0/2$ @$\Delta x=2X_0$ e $\rightarrow \gamma$ e' $E'=E_0/4$

@$\Delta x=tX_0$ $N(t) = 2^t$ $E(t) = E_0 / 2^t$

@ $t_{max}X_0$ (shower max) $E(t_{max}) = E_c$ $E_0 / 2^{t_{max}} = E_c$

$t_{max} = \ln(E_0/E_c)/\ln(2)$

$$N_{TOT.} = \sum_{t=0}^{t=t_{max}} 2^t = 2^{(t_{max}+1)} - 1 \approx 2 \cdot \frac{E_0}{E_C}$$

EM showers – Longitudinal profile

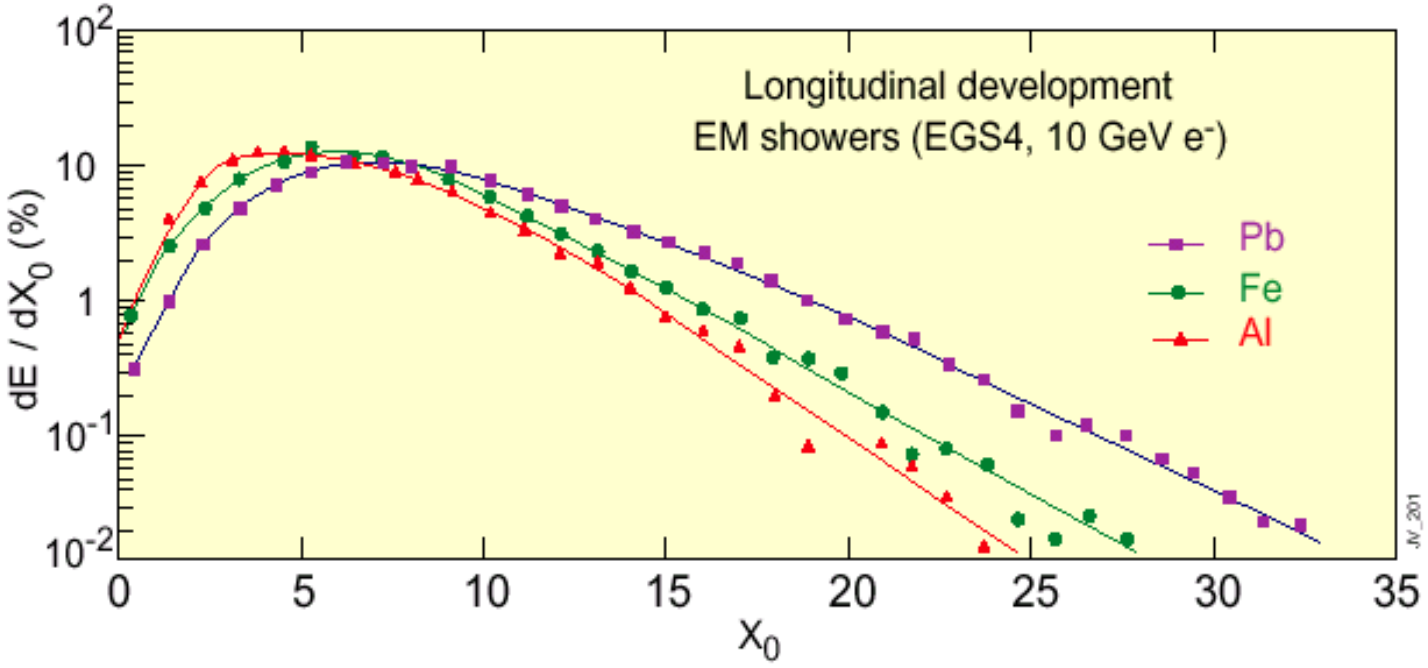

$$\frac{dE}{dt} \propto t^{\alpha} e^{-\beta t}$$

Longo e Sestili '75

Parametrization of energy deposition $N_{tot} \propto E_0/E_c \quad t_{max} = 1.4 \ln(E_0/E_c)$

Longitudinal containment $t_{95\%} = t_{max} + 0.08Z + 9.6$

$E_c \propto 1/Z$ ➡

- shower max
- shower tail

EM showers – Longitudinal profile

$$t_{max} = 1.4 \ln(E_0/E_c)$$

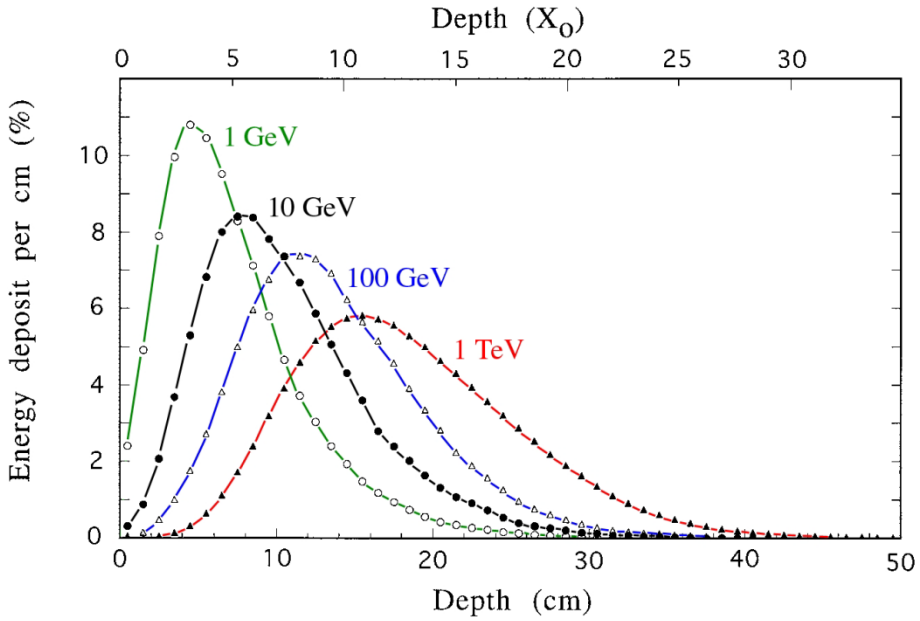

Electron shower in a block of copper

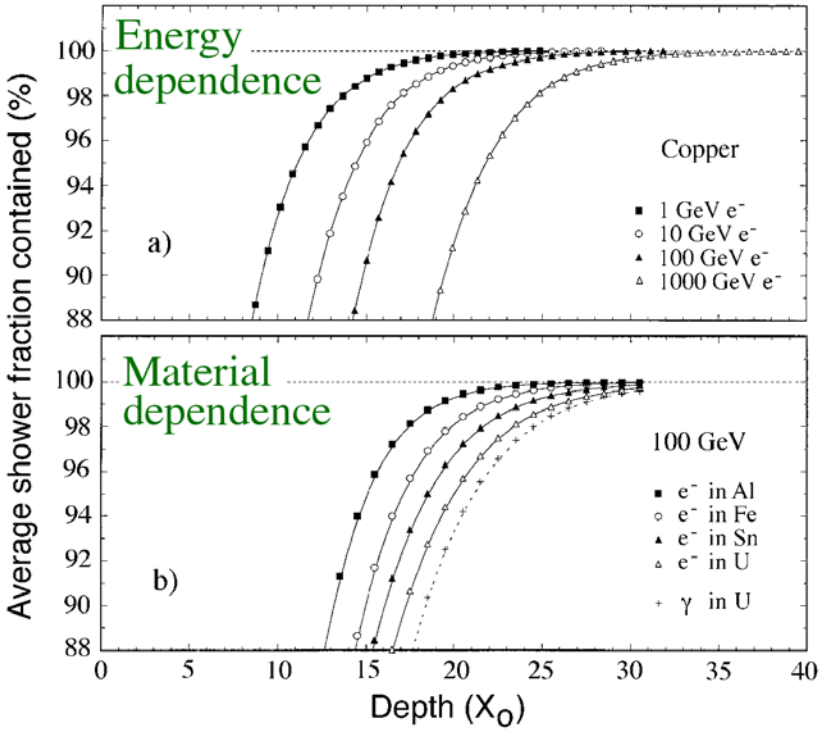

1 GeV electron in copper:
95% in 11 X_0 and 99% in 16 X_0
1 TeV electron in copper:
95% in 22 X_0 and 99% in 27 X_0

EM showers – Parametrizations

Transverse shower profile

- Multiple scattering make electrons move away from shower axis
- Photons with energies in the region of minimal absorption can travel far away from shower axis

Molière radius sets transverse shower size;
on average 90% of the shower is conteined within cylinder of radius R_M around the shower axis.

$$R_M = \frac{21\,MeV}{E_C} X_0$$

$$R_M \propto \frac{X_0}{E_C} \propto \frac{A}{Z} \left(Z >> 1\right)$$

90% E_0 within $1R_M$, 95% within $2R_M$, 99% within $3.5R_M$

EM showers – Parametrizations

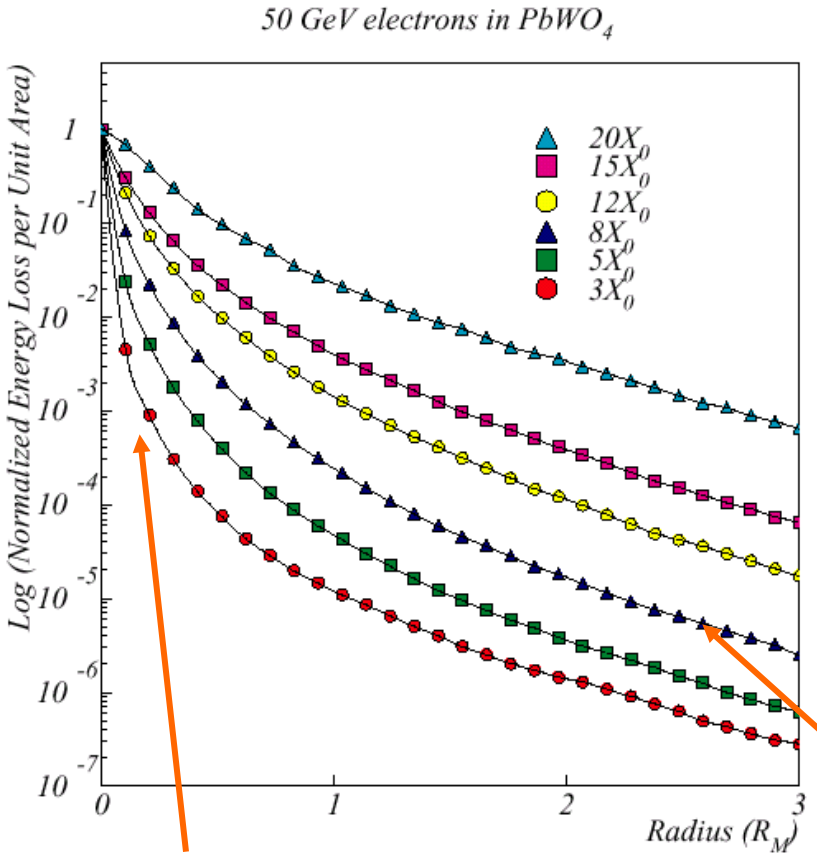

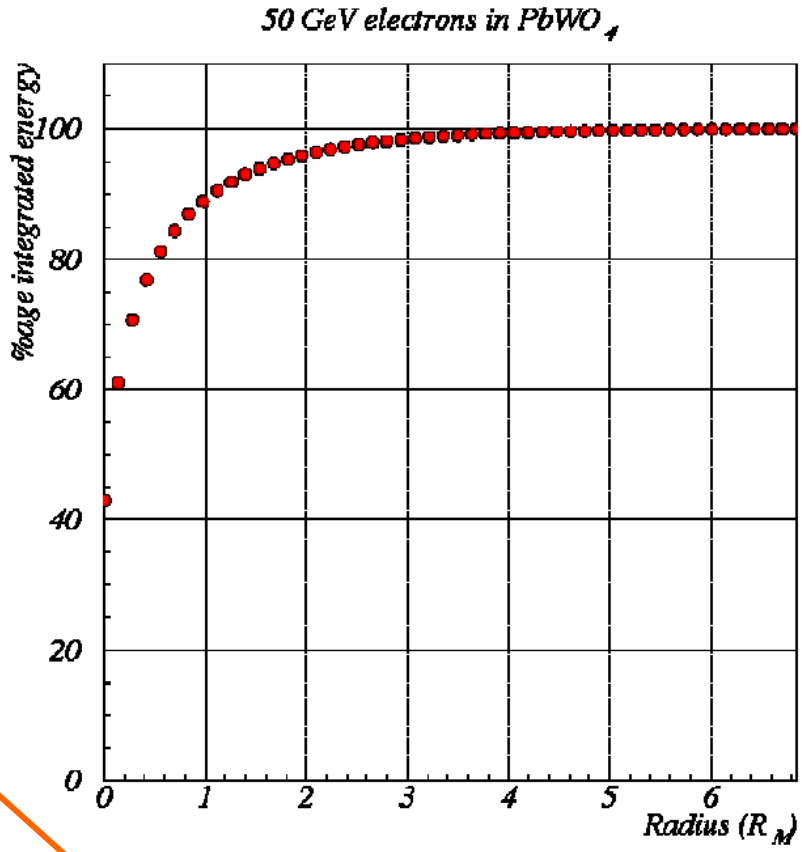

Central core: multiple scattering

Peripheral halo:
propagation of less attenuated photons,
widens with depth of the shower

Homogeneous and sampling calorimeters

- In homogeneous calorimeters the absorber and the active medium are the same (e.g. ECAL in Opal, L3, Babar and CMS)
- In sampling calorimeters the two roles are played by two different media (e.g. ECAL in Delphi and Atlas, HCAL in CMS).
  - Shower is sampled by layers of active medium (low-Z) alternated with dense radiator (high-Z) material.
  - Limited energy resolution
  - Detailed shower shape information
  - Reduced cost

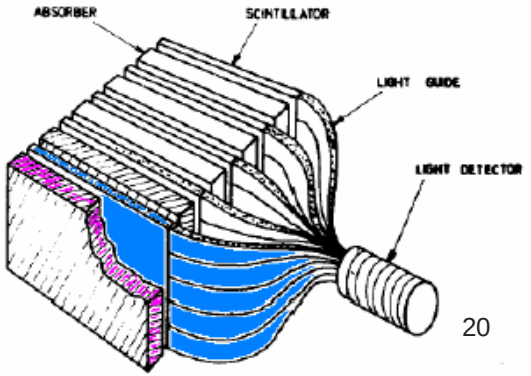

Electromagnetic showers in sampling calorimeter

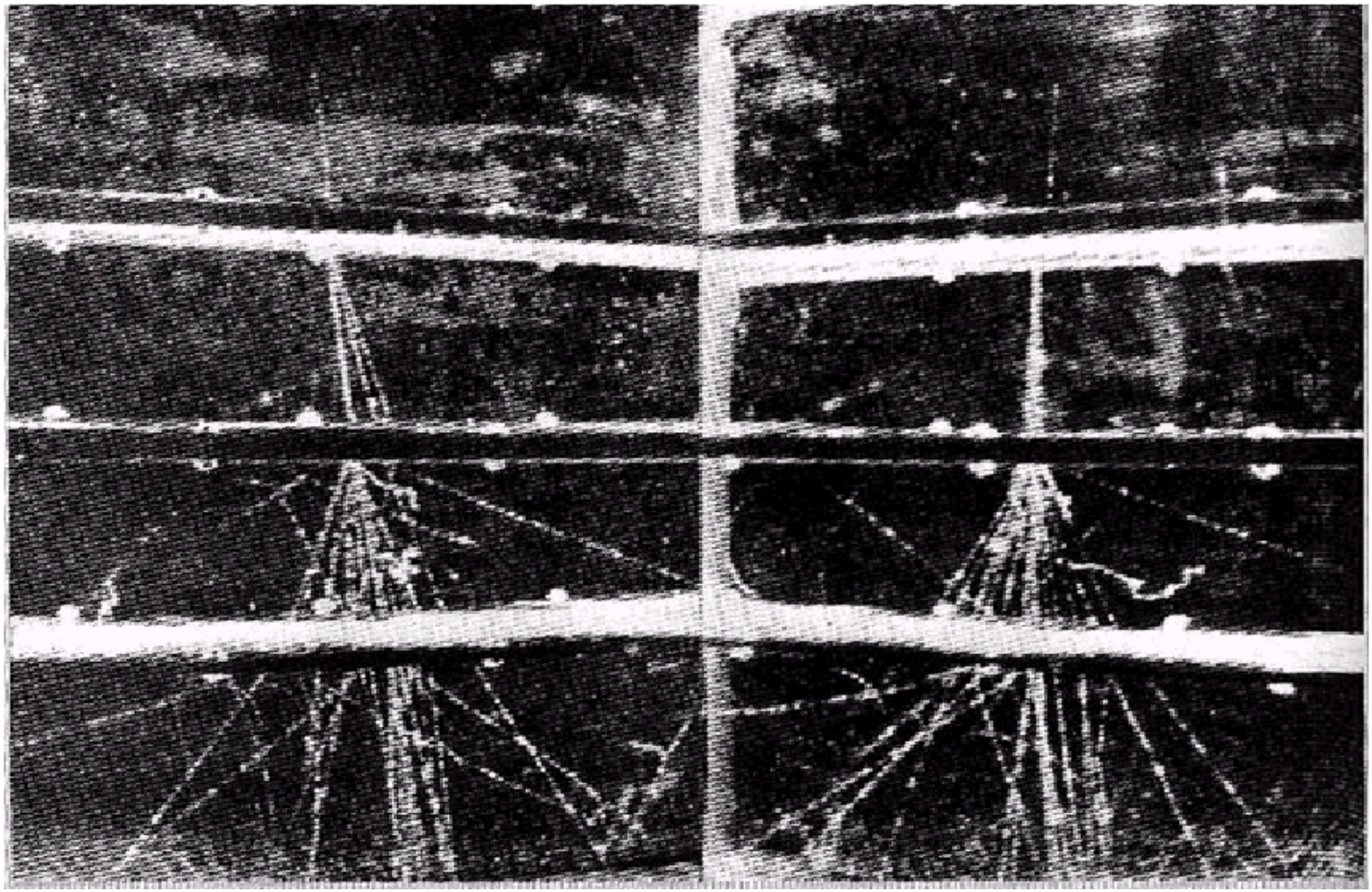

Cloud chamber photograph of e.m. shower developing
in lead plates exposed to cosmic radiation

Hadronic Showers

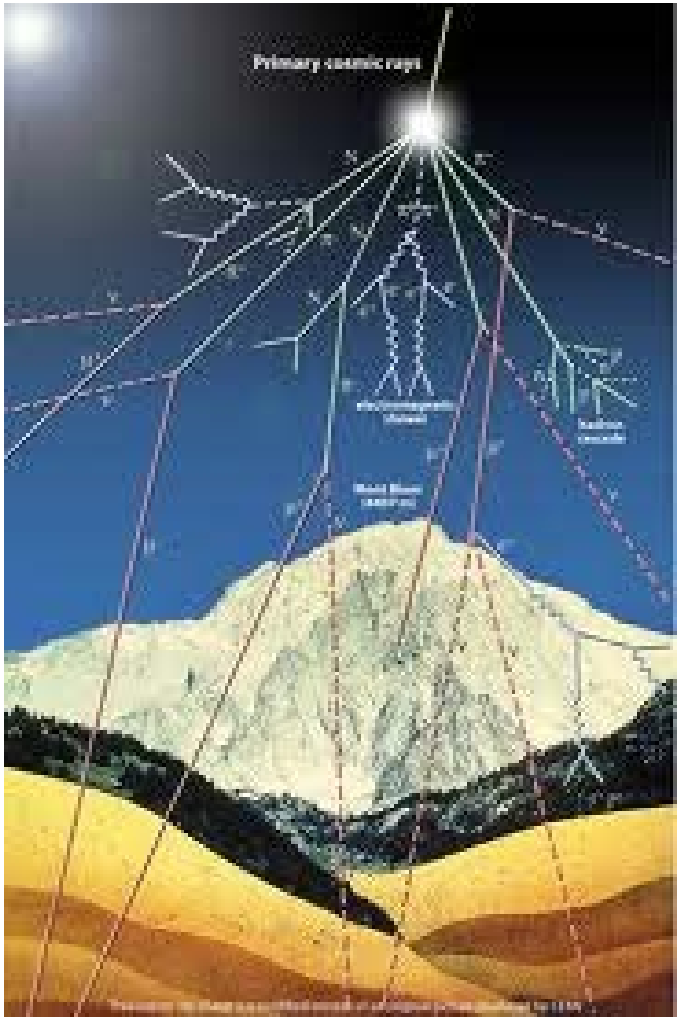

- A very popular hadronic shower.

Hadronic Showers

- Typical scale is the interaction length λ
- Good containment in ~10 λ but $\lambda > X_0$ (or $\lambda >> X_0$)
- Larger size of the calorimeters drives the choice of sampling HCAL

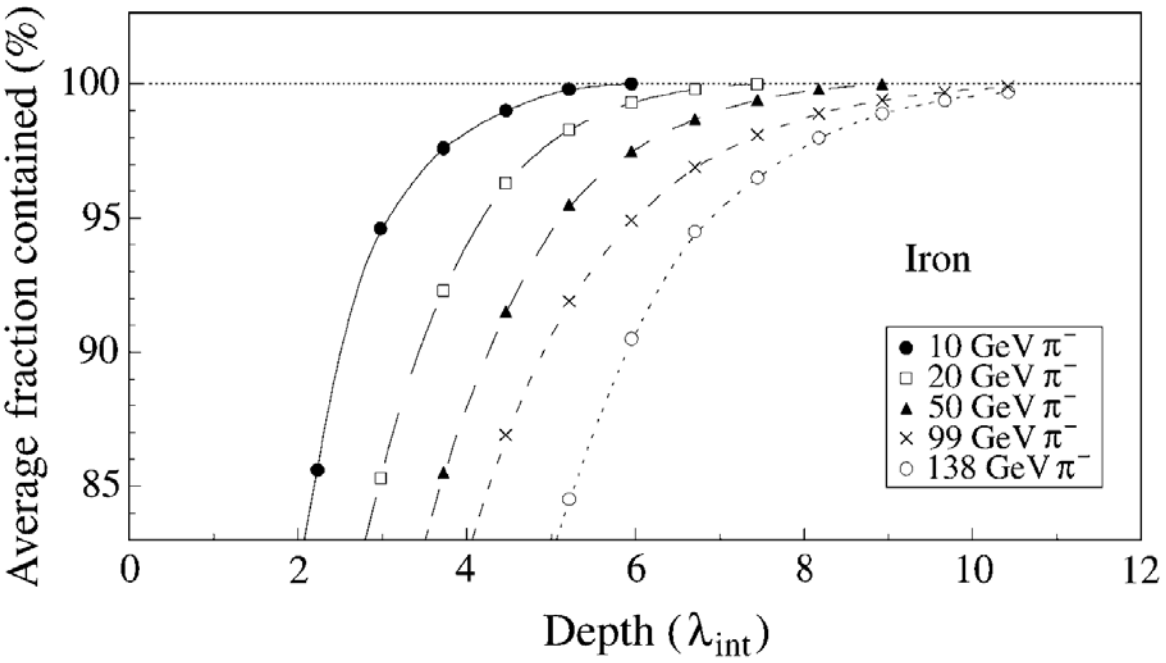

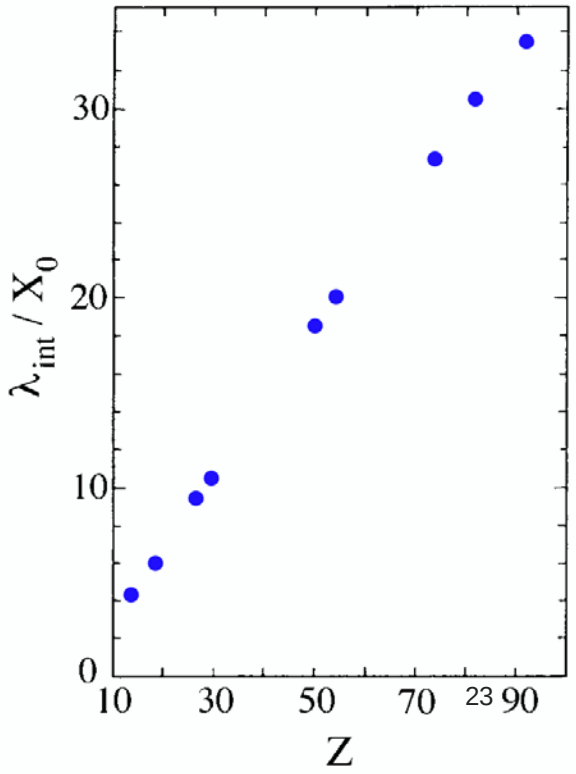

Hadronic Showers

- More complicated that em shower due to the presence of strong interaction.
- Pions (charged and neutral) are by far the most important contribution in the hadronic shower composition but the large majority of the energy is deposited through protons and neutrons.

Neutral pions decay in photons before to interact

→ electromagnetic component in the hadronic shower

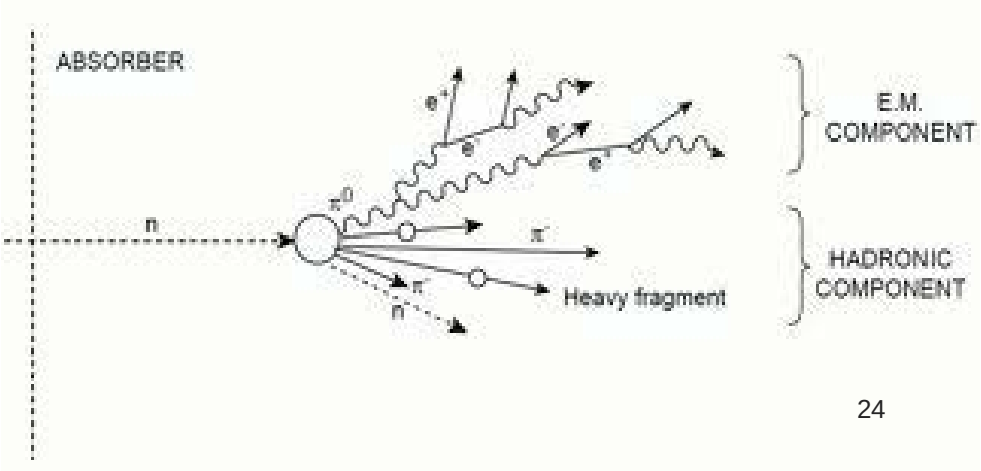

Hadronic Showers

- Big fluctuation in the hadronic shower profile and in the electromagnetic component size.
- Energy dependence of electromagnetic component
- Both the effects strongly affect the calorimeter performance

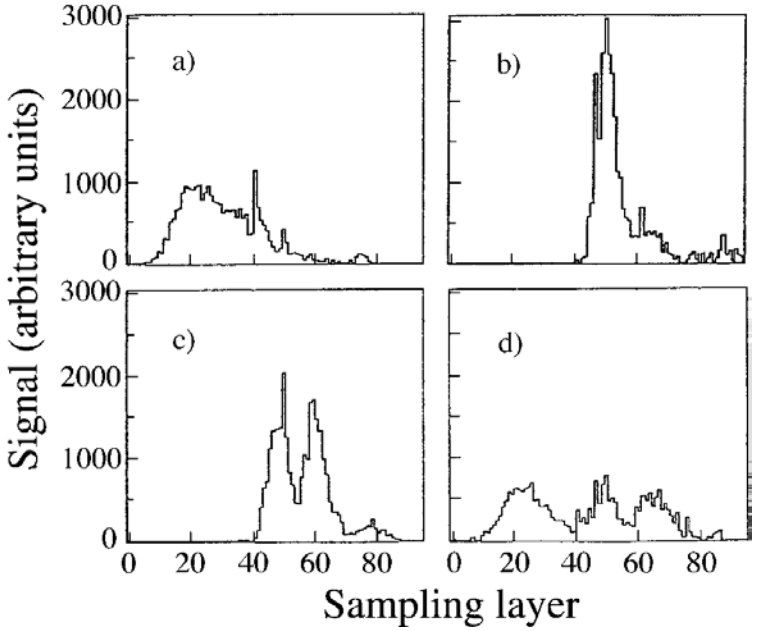

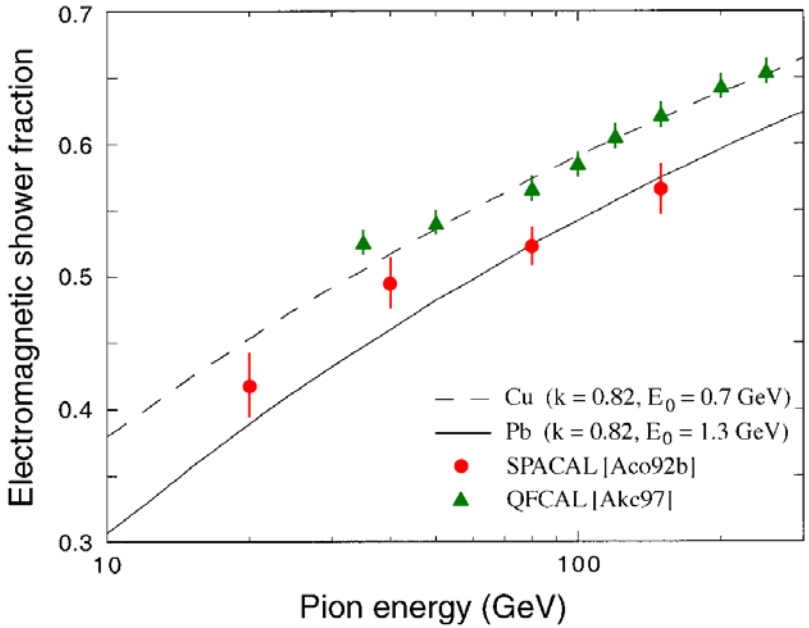

Hadronic Showers

- A not negligible fraction of hadronic energy does not contribute to the calorimeter signal (e/h>1):
  - energy to release nucleons from nuclei
  - muons and neutrinos from pi/K decays
- The calorimeter response to hadrons is generally smaller than to electrons of the same energy (**π/e < 1**).
- Degradation in energy resolution (the energy sharing between em and non-em components varies from one event to another) and linearity (the em fraction of hadron-induced showers increases with energy, so π/e does).

Compensation

Compensation: equalization of the response to the electromagnetic and non-em shower components (e/h = 1).

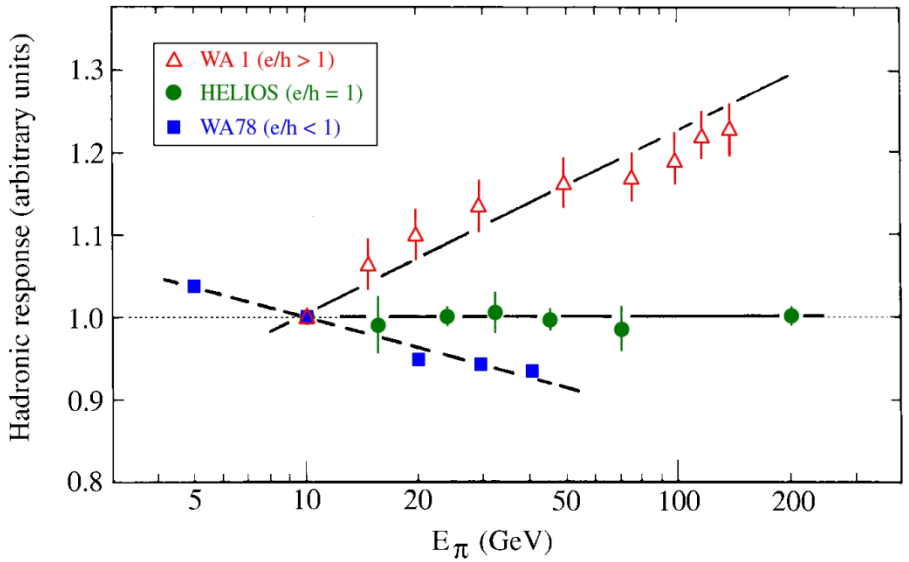

$$\frac{e}{\pi} = \frac{e/h}{1 - f_{\mathrm{em}}(1 - e/h)}$$

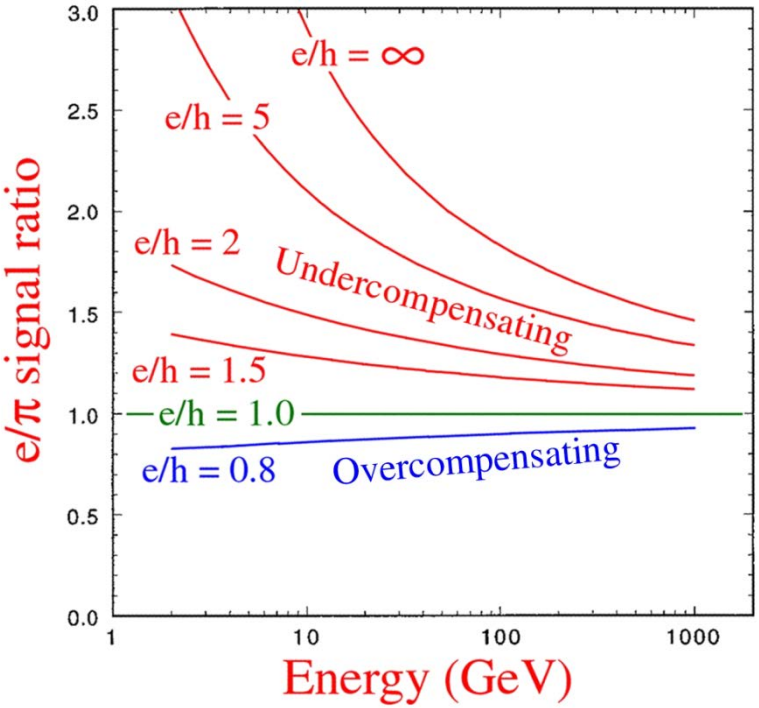

Energy Flow

- Measure charged particles with tracker, photons with ECAL and neutral hadrons with HCAL.
- Fine granularity

Intensively used in CMS
Strong benefit on Jet and Met resolution.

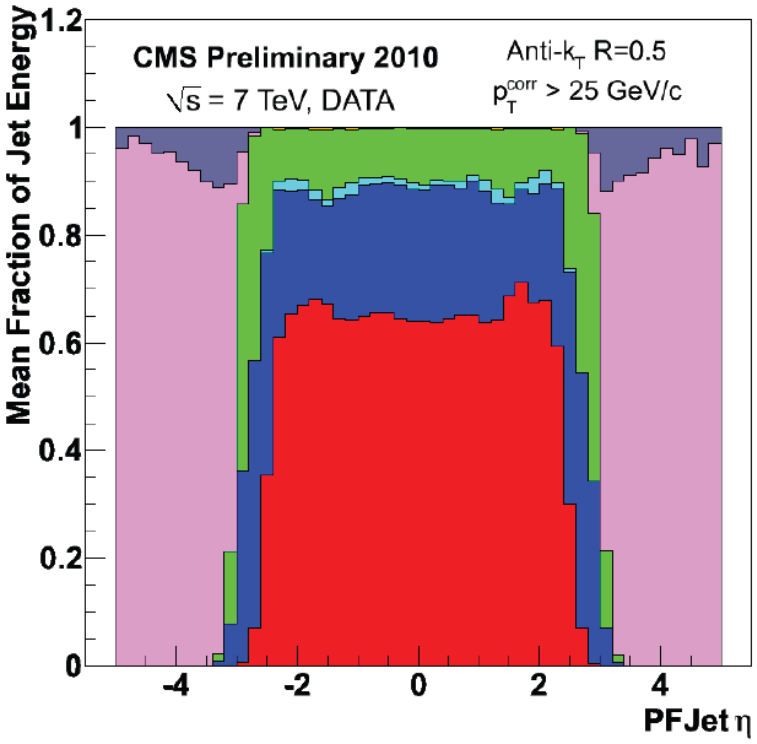

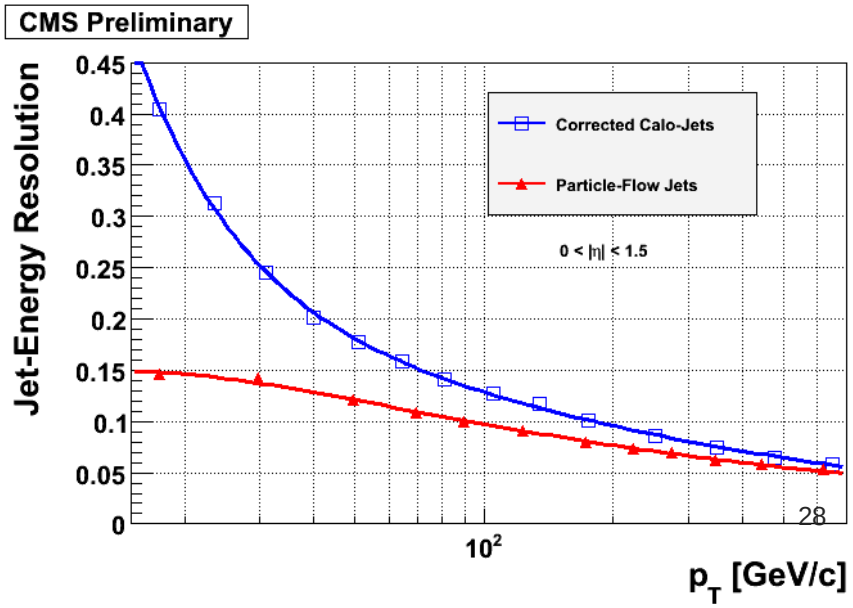

EM showers – Energy loss detection

The energy deposited in the calorimeters is converted to active detector response

- $E_{vis} \leq E_{dep} \leq E_0$

Main conversion mechanism

- Cerenkov radiation from $e^{\pm}$
- Scintillation from molecules
- Ionization of the detection medium

response $\propto$ total track length

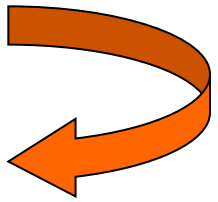

Different energy threshold E_s for signal detectability

Scintillators

Luminescent materials emit light when stimulated with light and heat (photo-luminescence) and radiation (scintillation). Two classes: organic and inorganic scintillators.

Inorganic (crystalline structure)	Organic (plastics or liquid solutions)
Up to 40000 photons per MeV	Up to 10000 photons per MeV
High Z	Low Z
Large variety of Z and ρ	$\rho \sim 1 gr/cm^3$
Undoped and doped	Doped, large choice of emission wavelength
ns to μs decay times	ns decay times
Expensive	Relatively inexpensive
E.m. calorimetry (e, γ)	Tracking, TOF, trigger, veto counters, sampling calorimeters.
Medical imaging	
Fairly Rad. Hard (100 kGy/year)	Medium Rad. Hard (10 kGy/year)

Scintillation mechanism

Scintillators need impurities (dopant) in order to emit at a different wavelenght and not reabsorb the light.

The centres are of three main types:

- Luminescence centres
  photon emission
- Quenching centres
  thermal dissipation of the excited energy
- Traps
  metastable levels, from where electrons may subsequently go to
  - conduction band by thermal energy
  - valence band by a radiationless transition

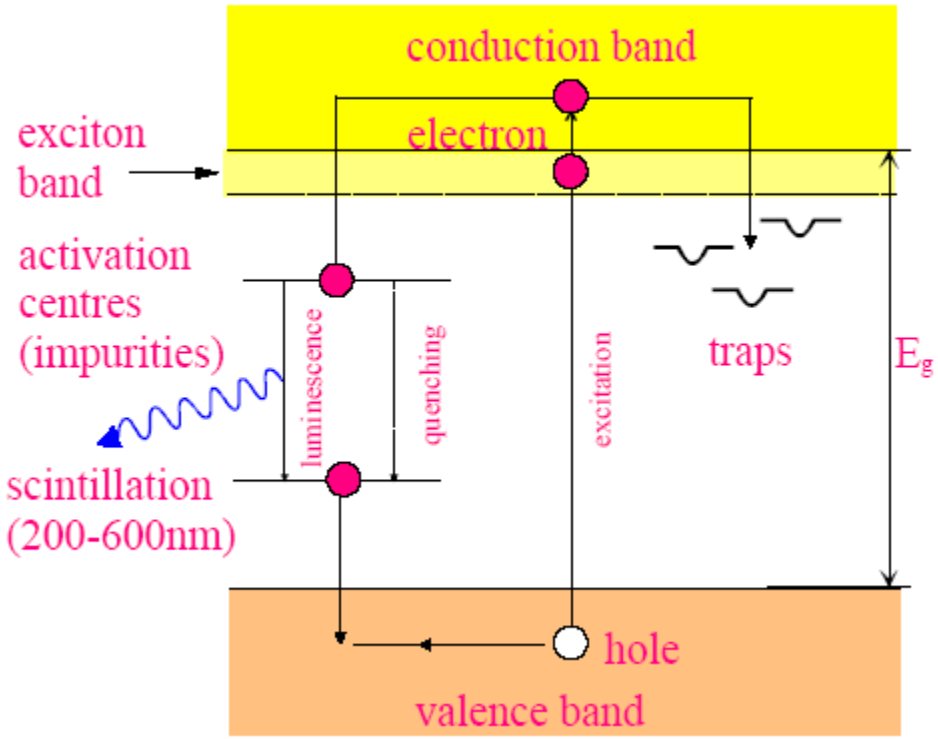

Scintillating Crystal History

Among different types of calorimeters those with scintillating crystals are the most precise in energy measurements

- Discovery and development of new scintillators driven by basic research and technology in physics

- HEP has played a major role in developing new scintillators at an industrial scale and affordable cost, e.g. BGO, CsI, $PbWO_4$.

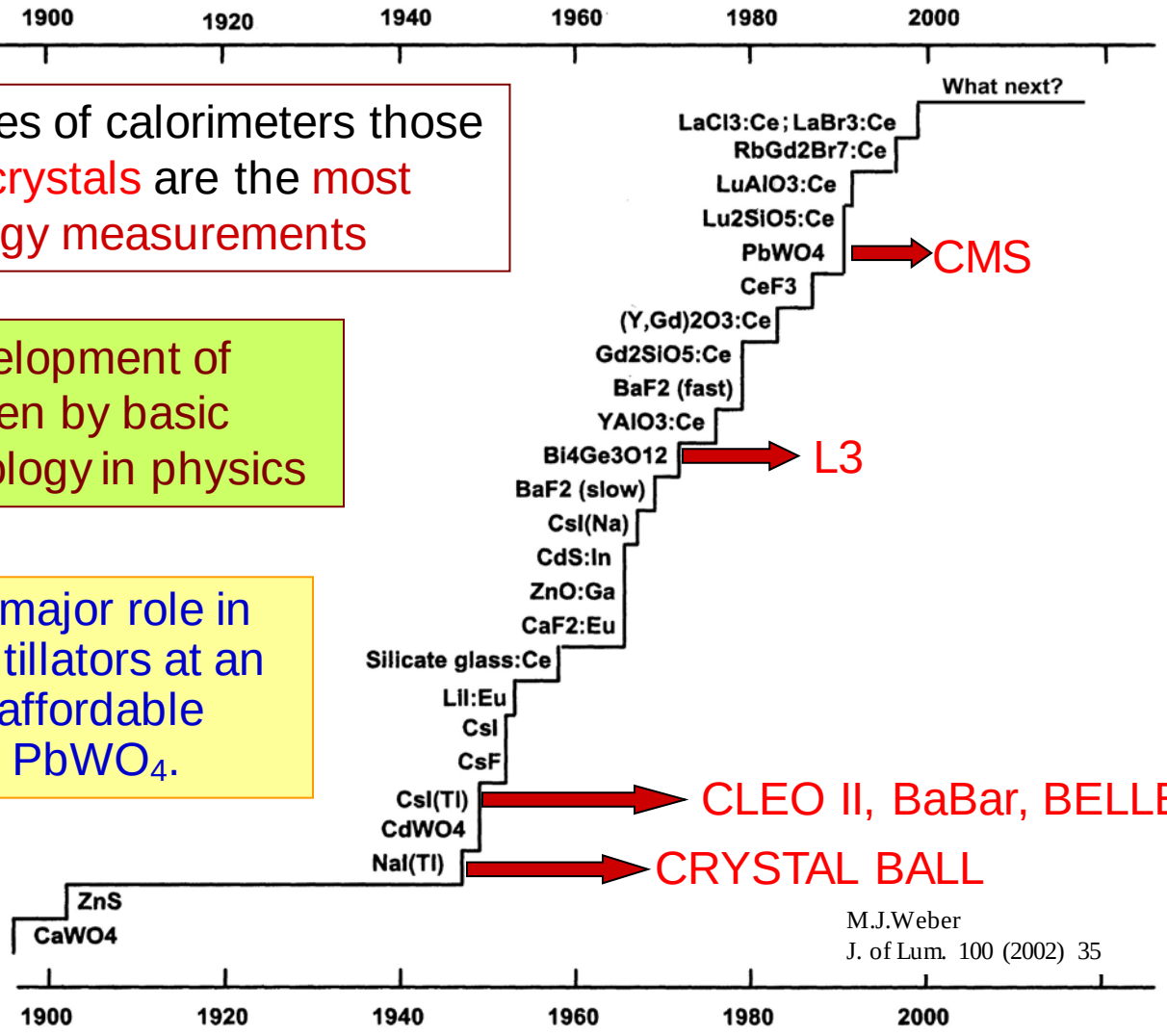

Cherenkov Light

- A charged particle traveling in matter with speed greater than c/n (the speed of the light in the same material) emits photons mainly in the visible (mainly in the blue).

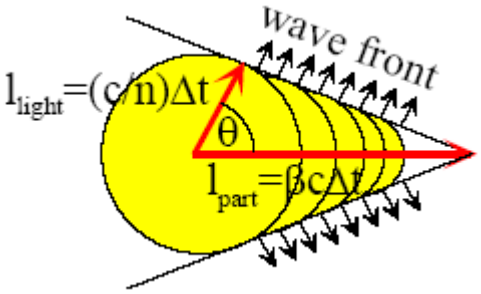

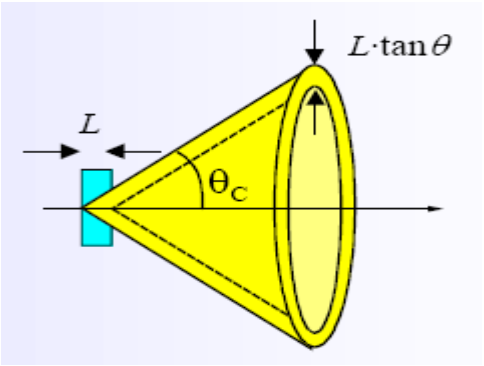

Maximum value for the emission angle (v=c)

$$\theta_{max} = \arccos\frac{1}{n}$$

- The energy loss by Cherenkov effect is much smaller that the energy loss by ionization: high gain photodetector is needed (e.g. PMTs)

Energy Resolution (1)

$$\frac{\sigma}{E} = \frac{s}{\sqrt{E}} \oplus c \oplus \frac{n}{E}$$

$\oplus$ means quadratic sum

- s: stochastic term from Poisson-like fluctuations
  - sampling contribution dominant in sampling calorimeters
- c: constant term
  - dangerous limitation to high energy resolution
  - important contribution from intercalibration constants
- n: noise term from electronic and pile-up
  - relevant at low energy

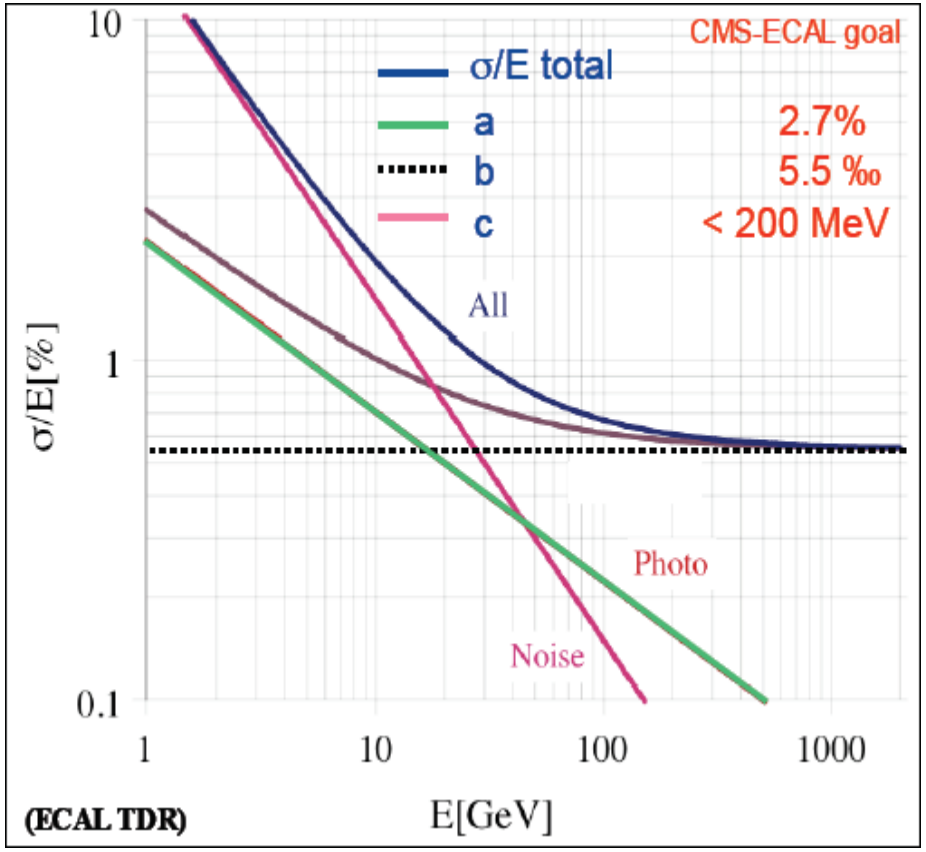

Energy Resolution (2)

- S: stochastic term from Poisson-like fluctuations
  (natural advantage of homogenous calorimeters; s can be ~ 2%-3%)

  • photostatistics contribution:
    - light yield
    - geometrical efficiency of the photodetector
    - photocatode quantum efficiency

  • electron current multiplication in photodetector

  • lateral containment of the shower

  •Material in front of the calorimeter

$$E \propto N_{\text{p.e.}}$$

$$\sigma(N_{\text{p.e.}}) \propto \sqrt{N_{\text{p.e.}}}$$

$$\Rightarrow \quad \frac{\sigma(E)}{E} \propto \frac{1}{\sqrt{E}}$$

Including gain fluctuations of photo-detector (F) :

$$\frac{\sigma(E)}{E} = \sqrt{\frac{F}{N_{\text{p.e.}} \cdot E}}$$

$$F = 2-3; \quad N_{\text{p.e.}} \geq 4000/\text{GeV}$$

Energy Resolution (3)

Constant Term contributions in CMS ECAL:

- leakage (front, rear, dead material)
- temperature stabilization < 0.1 °C
  (dLY/dT = -2.0%/°C @ 18°C ;
  dM/dT ~ -2.3 %/°C)
- APD bias stabilization (±20 mV / 400 V)
  (dM/dV = 3%/V)
- light collection uniformity
- intercalibration by light injection monitor and physics signals

Light Collection Uniformity

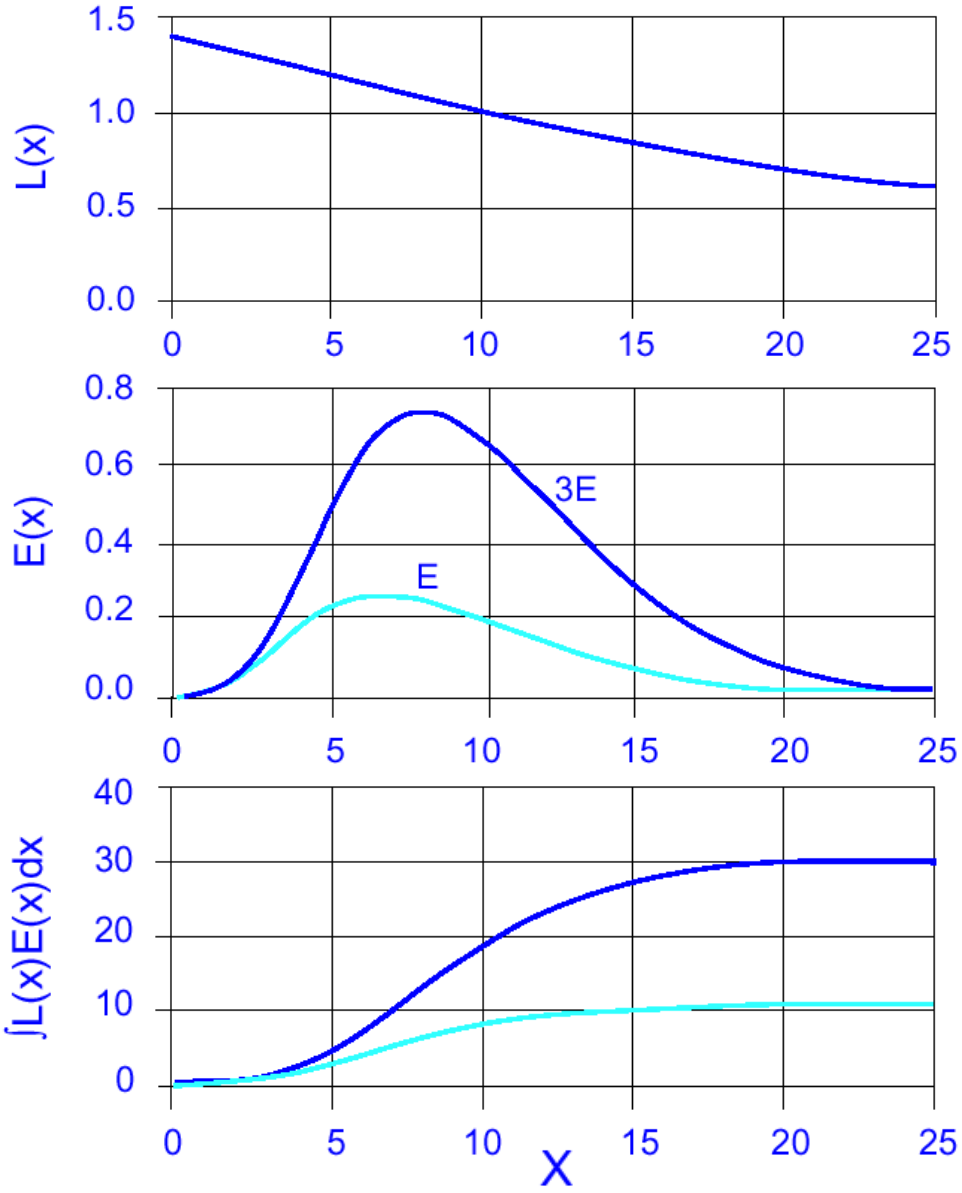

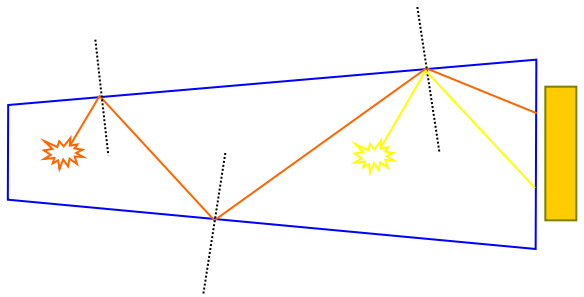

- non linearity of the response (can be corrected)
- smearing of the response at fixed energy due to shower fluctuations (can not be corrected)

$$\int_0^x L(x)E(x)dx$$

ratio 2.89
(instead of 3)

Light Collection Uniformity

- High refractive index make light collection difficult
- Focusing effect due to tapered shape of barrel crystals
- Uniformity can be controlled by depolishing one lateral face with a given roughness

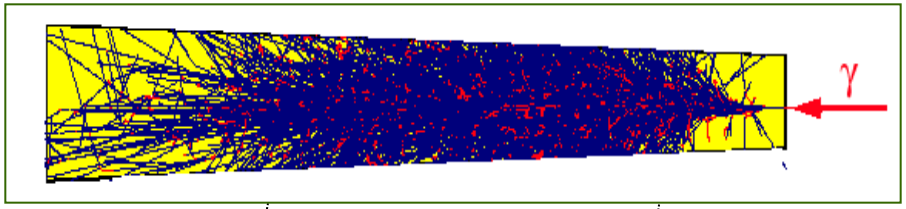

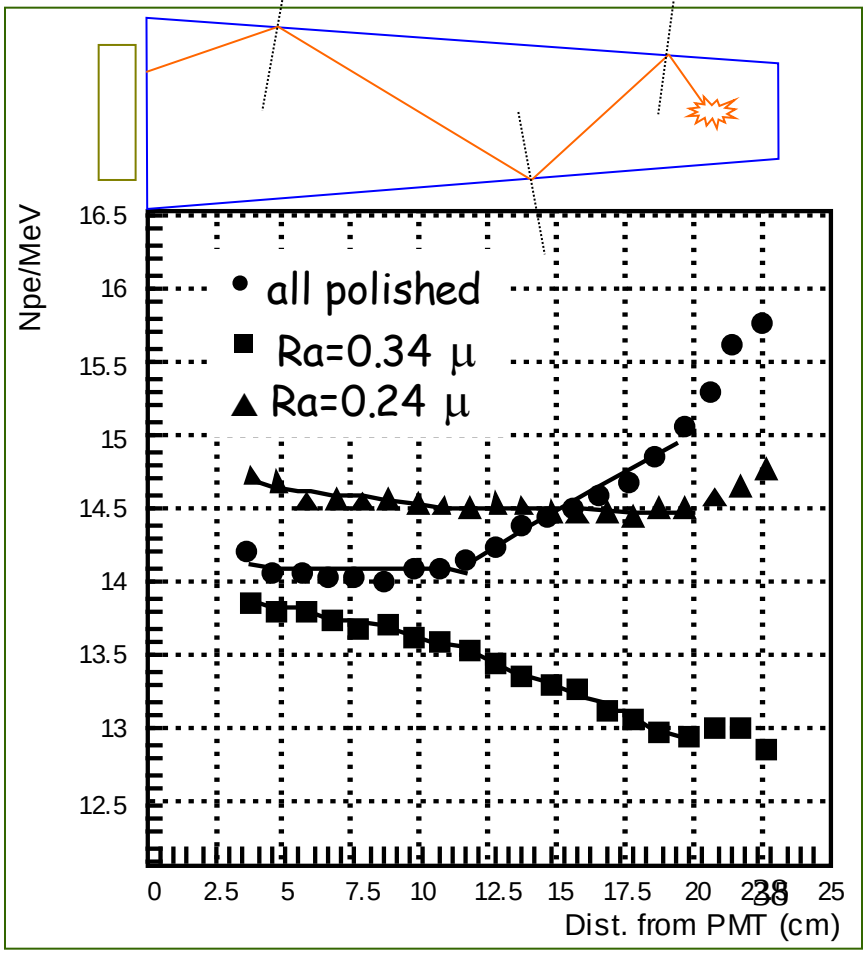

Uniformity treatment

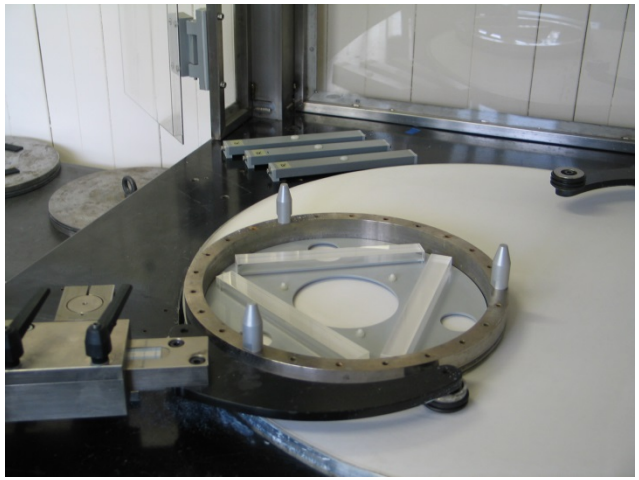

The CMS calorimeters

Disclaimer: due to the limited time, I selected few "ECAL oriented" examples to show the performance in CMS.

Plots from the CMS paper EGM-11-001

http://m.iopscience.iop.org/1748-0221/8/09/P09009

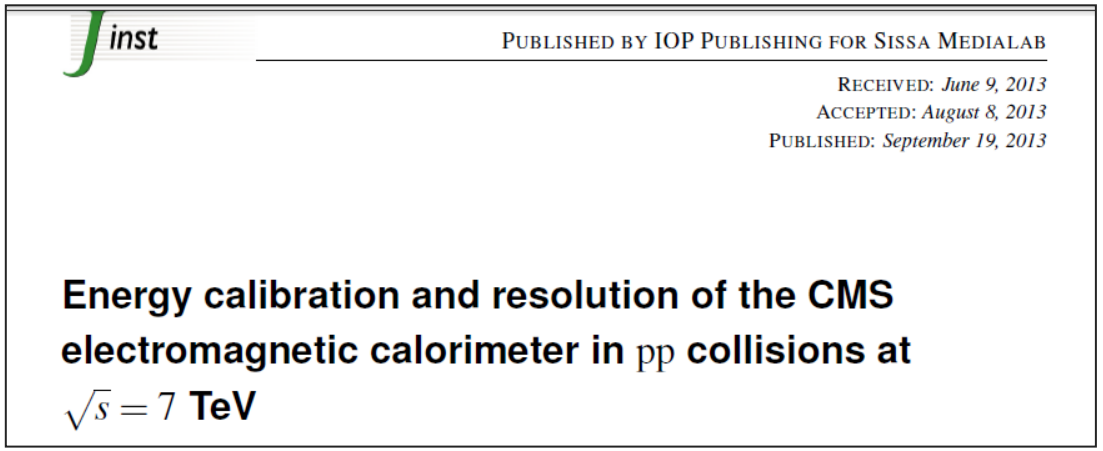

CMS Hadronic Calorimeter

- Hadronic Barrel (HB) and Endcap (HE) calorimeters:
  - sampling brass/plastic scintillator tiles
  - HO: additional scintillator layer outside the solenoid cryostat
- The forward calorimeter (HF):
  - steel and quartz fiber covers up to $|\eta|<5.2$

  - old russian shell casings recycled for brass !

CMS Hadronic Calorimeter

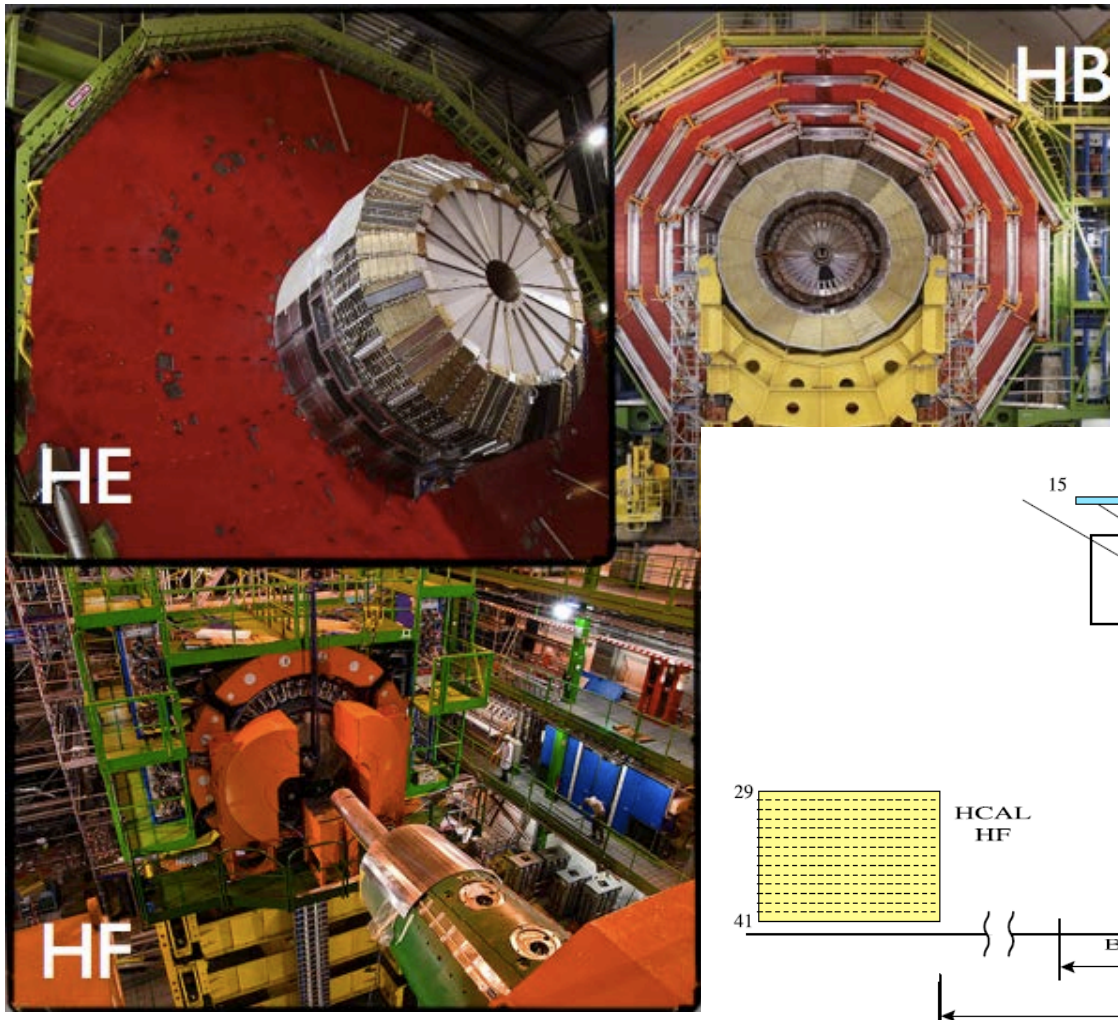

Detector	Readout	# Channels
HB/HE/HO	Hybrid Photo-Diode (HPD)	2592/2592/2160
HF	PMT	1728

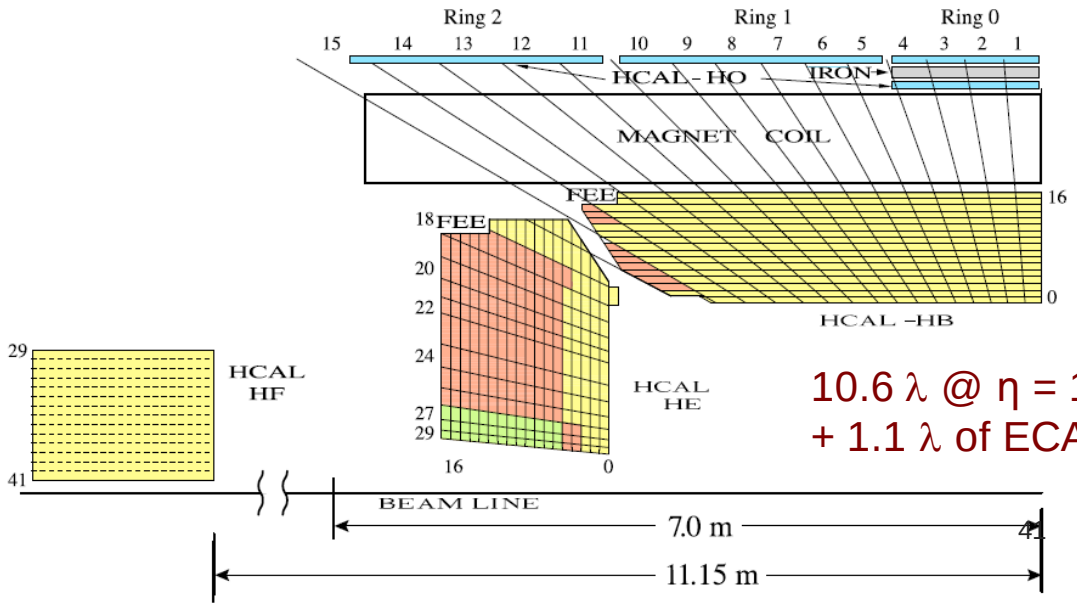

10.6 λ @ η = 1.3
+ 1.1 λ of ECAL

CMS Electromagnetic Calorimeter

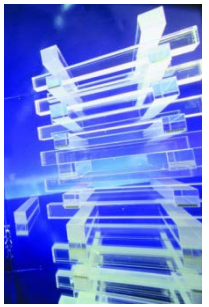

- Excellent energy (and position) resolution for photons and electrons ($H\rightarrow\gamma\gamma$, $H\rightarrow ZZ \rightarrow 4e$)
- Lead Tungstate ($PbWO_4$) homogenous crystal calorimeter
- Barrel (EB):
  - 36 Supermodules (SM), each 1700 crystals
  - $|\eta|<1.48$
  - APD photodetectors
- Endcaps (EE):
  - 2 Endcap sides, each 7324 crystals
  - $1.48<|\eta|<3.0$
  - VPT photodetectors
- Preshower (ES):
  - sampling calorimeter (lead, silicon strips)
  - $1.65<|\eta|<2.6$

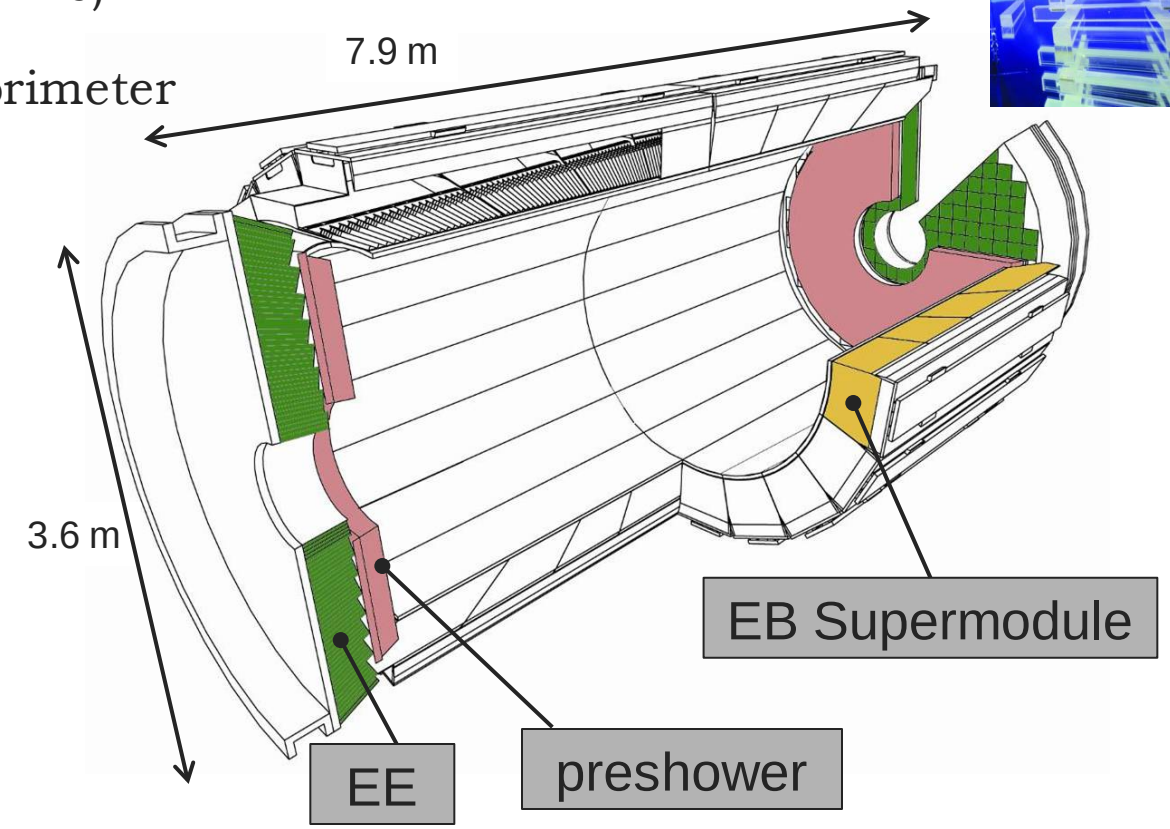

Pre-calibration Campaign

A very intense 10 years long pre-calibration campaign. Several orders of magnitude in energy: from 1 MeV of Co^{60} source to 120 GeV electron beam.

Laboratory measurements during crystal qualification phase.
(2000-2006)

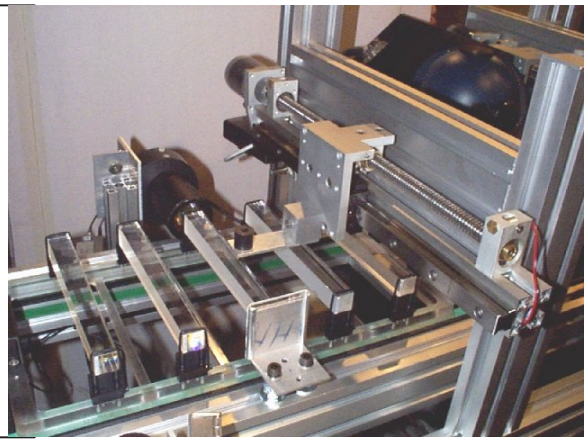

Test Beam:
Cern electron beams.

From 15 GeV to 250 GeV.
(2004-2007)

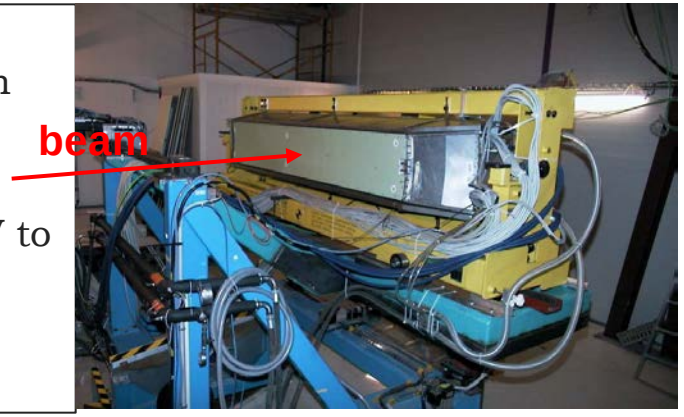

Channel intercalibration with cosmic muons (only Barrel SMs)

(2006-2007)

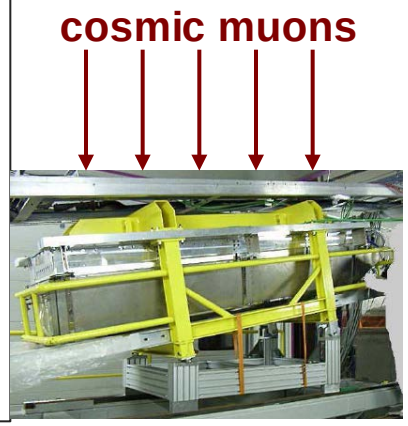

Beam Splash:
In September 2008 and November 2009, beam was circulated in LHC, stopped in collimators 150m away from CMS

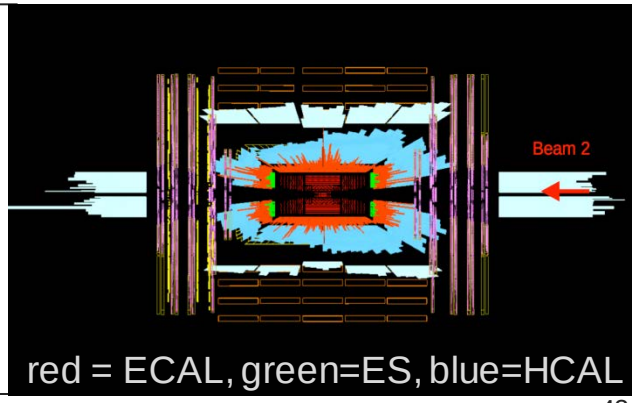

Energy resolution challenge

- ECAL «standalone» energy resolution measured at the test beam:
  (3x3 arrays of barrel crystals in the absence of magnetic field, with no material in front of the calorimeter and negligible inter-calibration contribution in the constant term)

$$\frac{\sigma(E)}{E} = \frac{2.8\%}{\sqrt{E(\mathrm{GeV})}} \oplus \frac{0.128}{E(\mathrm{GeV})} \oplus 0.3\%$$

- Results used to tune MC simulation.
- In-situ, for unconverted photons with energies in the range of interest for physics analyses, ~100 GeV, the in-situ constant term dominates.
- Constant term in-situ strongly depends on the quality of the stability, calibration and monitoring.
- Asymptotically to be kept at ~0.5%

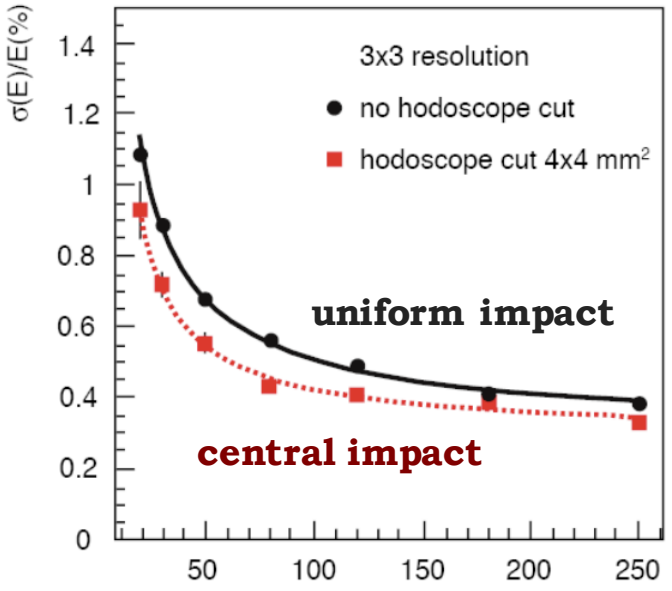

e/γ energy with ECAL

Measurement of electron/photon energy:

$$E_{e,\gamma} = F_{e,\gamma} \cdot \sum_{xtal} (G \cdot C_{xtal} \cdot L_{xtal}\,(t) \cdot A_{xtal})$$

- A_{xtal} [ADC counts] → signal channel amplitude
- L_{xtal} → laser monitoring correction (time dependent)
- C_{xtal} → crystal inter-calibration ($<C_{xtal}> = 1$)
- G [GeV/ADC] → ECAL energy scale
- Σ →e.m. shower, energy deposited over several crystals clustered with dynamic algorithms
- F → cluster energy corrections
  - particle dependent
  - compensate shower leakage and bremsstrahlung losses for electrons)

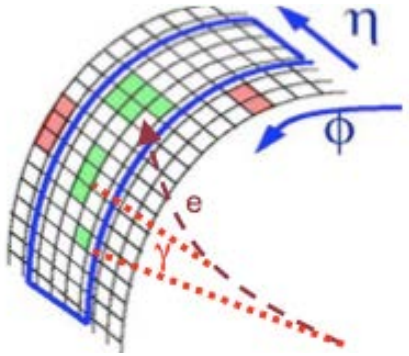

ECAL response monitoring

Radiation ⇨ Wavelength-dependent loss of light transmission (w/o changes in scintillation)

Crystal Transparency ***drops*** within a run by a few percent but ***recovers*** in the inter-fill periods

- Inject fixed amount of light to monitor transparency loss
- Response loss up to 5% in EB and up to 60% in EE (25% in the electron acceptance region $|\eta| < 2.5$)

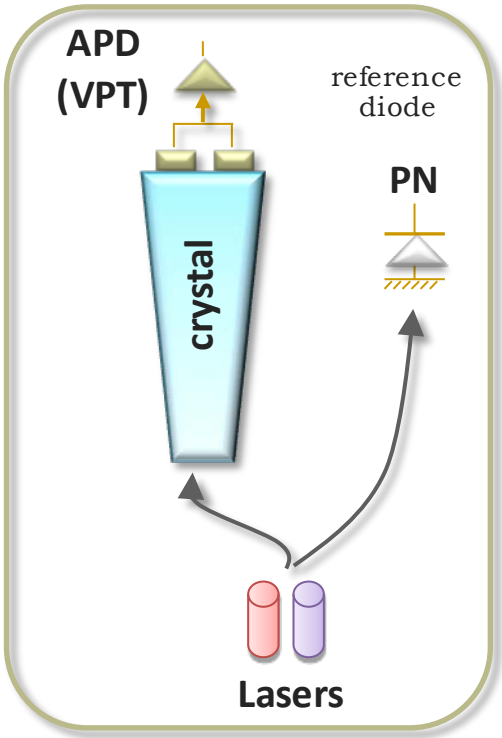

Cycle of response loss during irradiation and recovery in beam-off periods

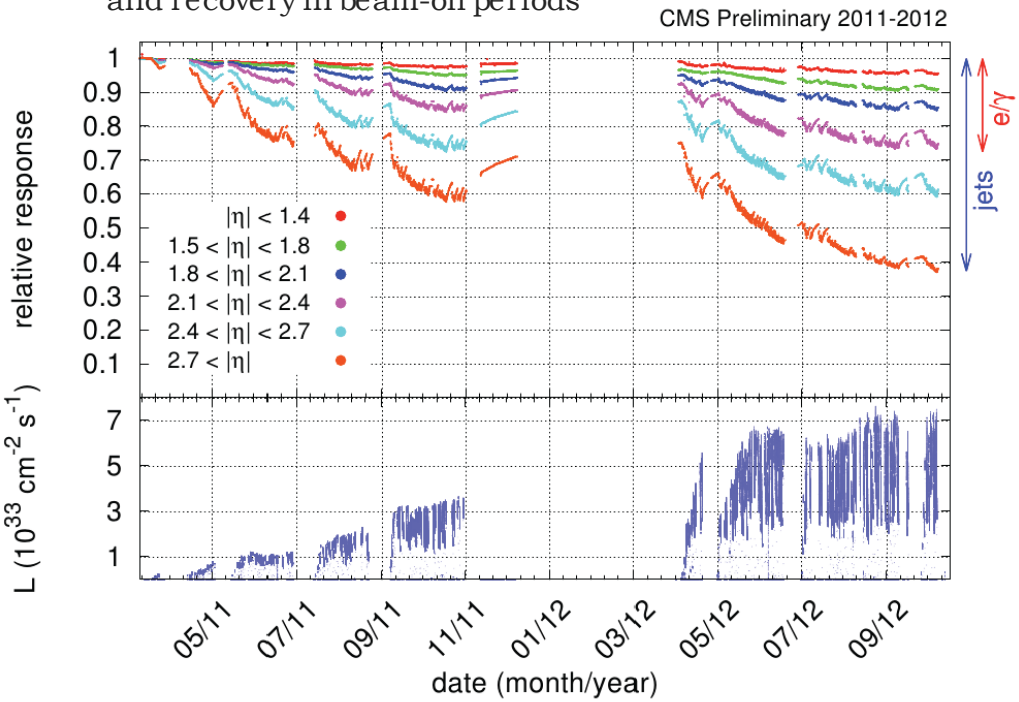

ECAL response stability

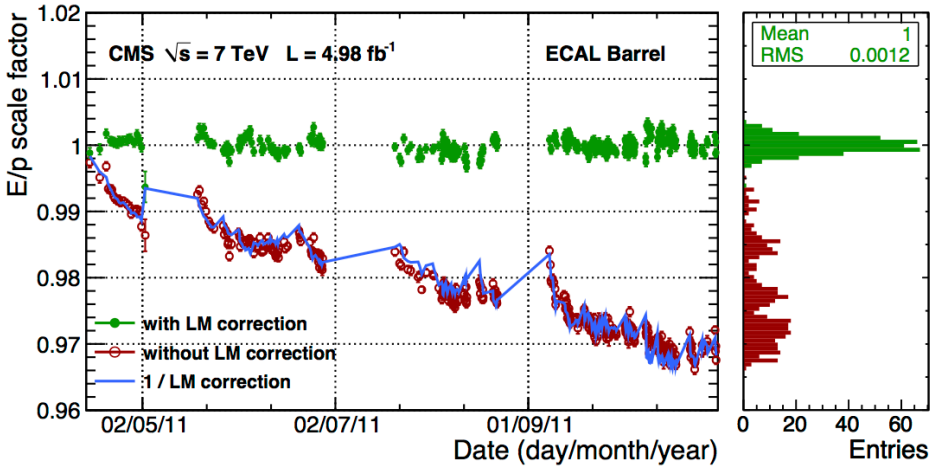

Stability (2011) of the energy scale after monitoring corrections with Wεν events.

- Barrel: average signal loss ~2.5%
  RMS stability ~0.12%
- Endcaps: average signal loss ~10%
  RMS stability ~0.35%

Stability of the ECAL resolution from Zee invariant mass peak.

- Barrel: resolution stable within errors.
- Endcaps: worsening of ~1.5% in quad. (residual PU effect)

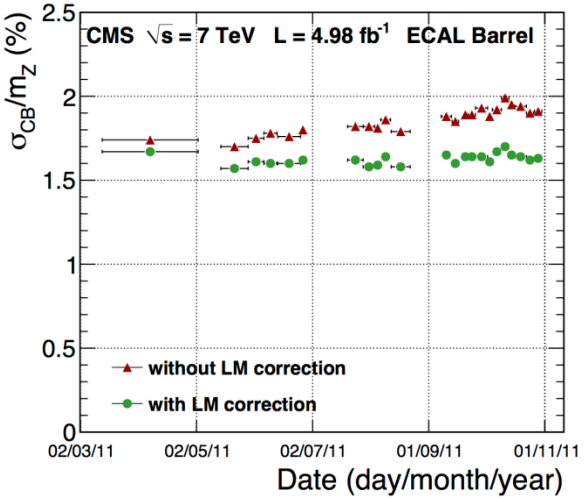

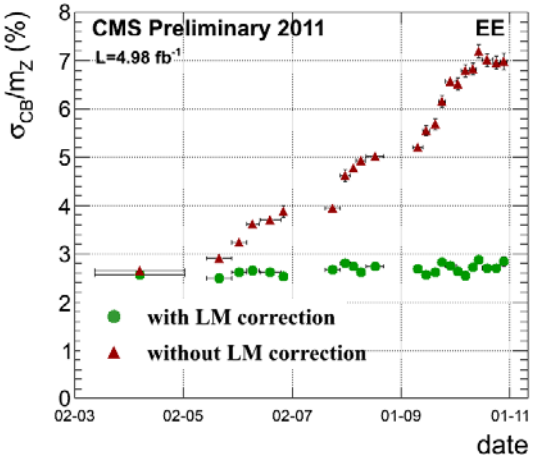

ECAL Calibration

- Zee invariant mass distribution applying :
  - channel Inter-Calibration
  - IC and Laser Monitoring corrections

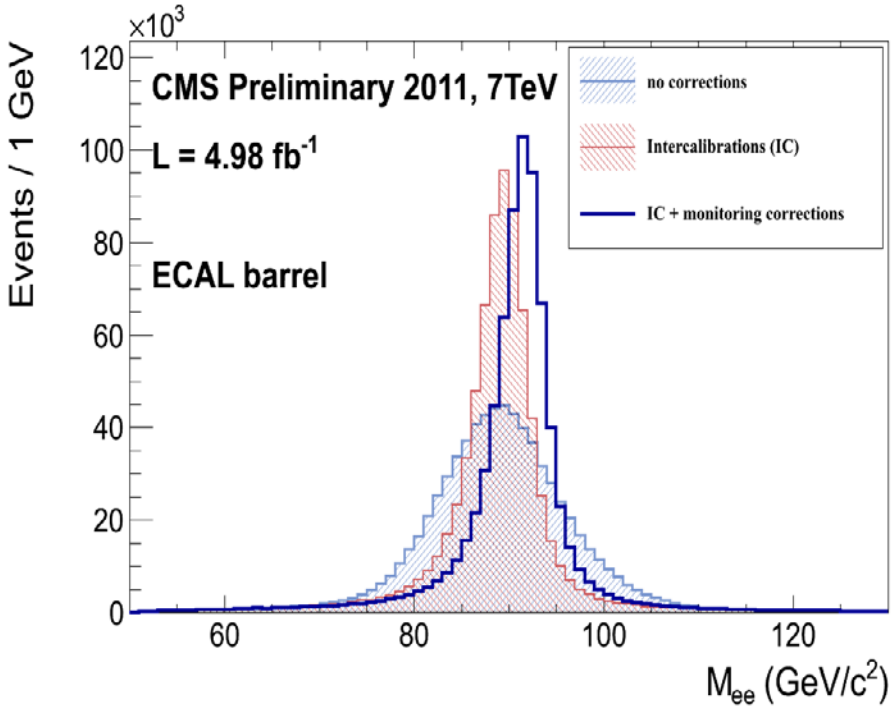

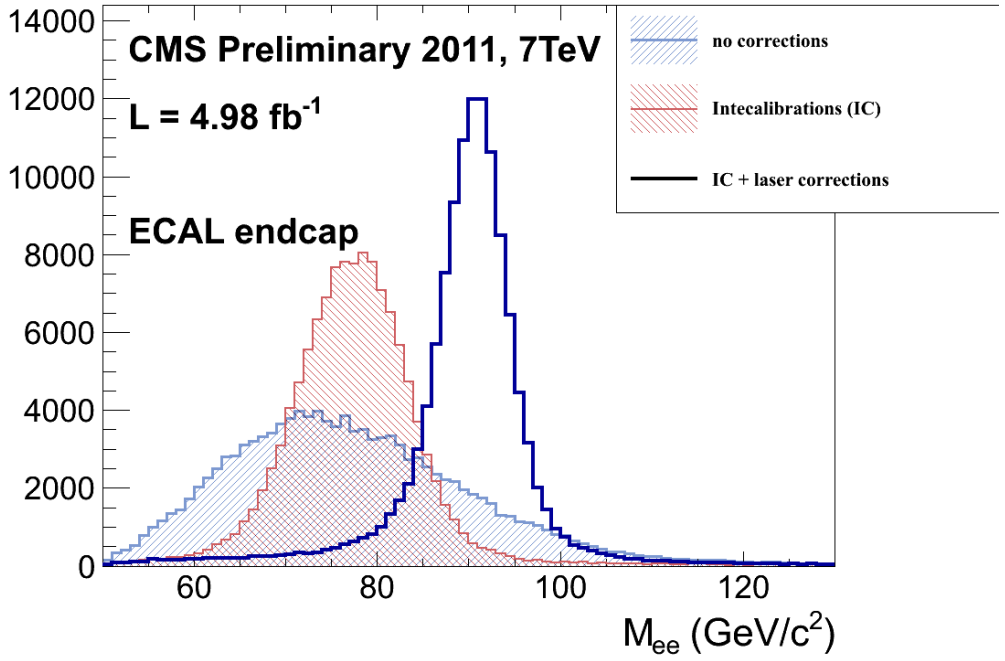

Cluster Energy Corrections

Cluster Energy corrections vs pseudo-rapidity for non-showering and showering electrons.

- compensate for unclustered energy and energy not reaching the calorimeter: strongly related to the amount of material in front of ECAL.
- energy lost inside gaps: intermodule boundary visible in the Barrel

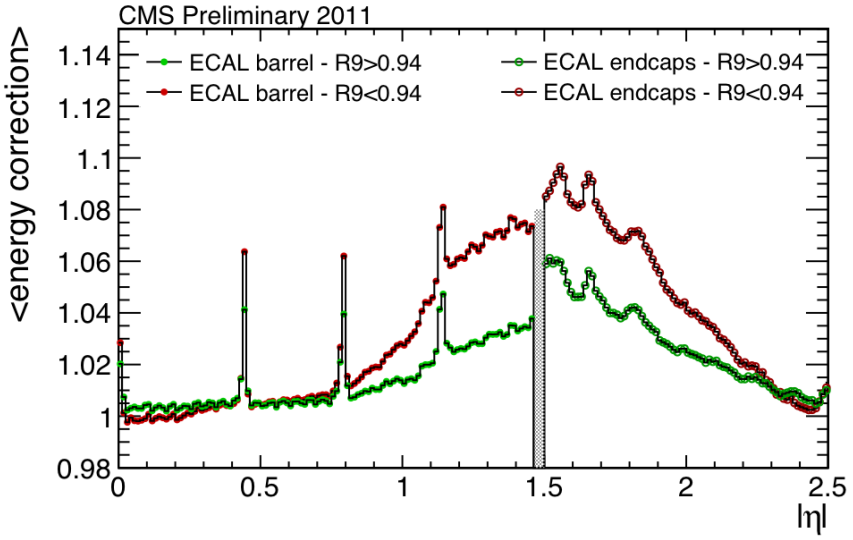

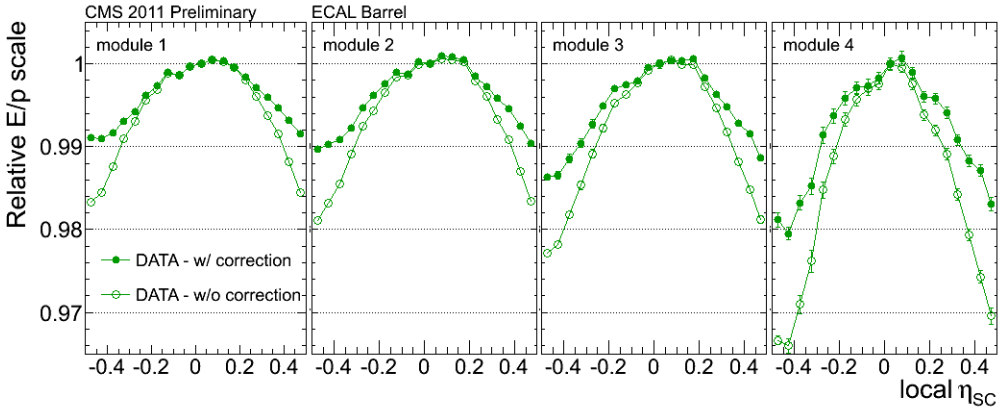

Reconstructed energy as a function of the local position of the most energetic crystal in the cluster, with E/p method.

- MC driven corrections not sufficient to correct the data
- crystal staggering variation along η (bigger in module 4)

Optimal clustering

- Zee invariant mass distribution with optimal ECAL clustering

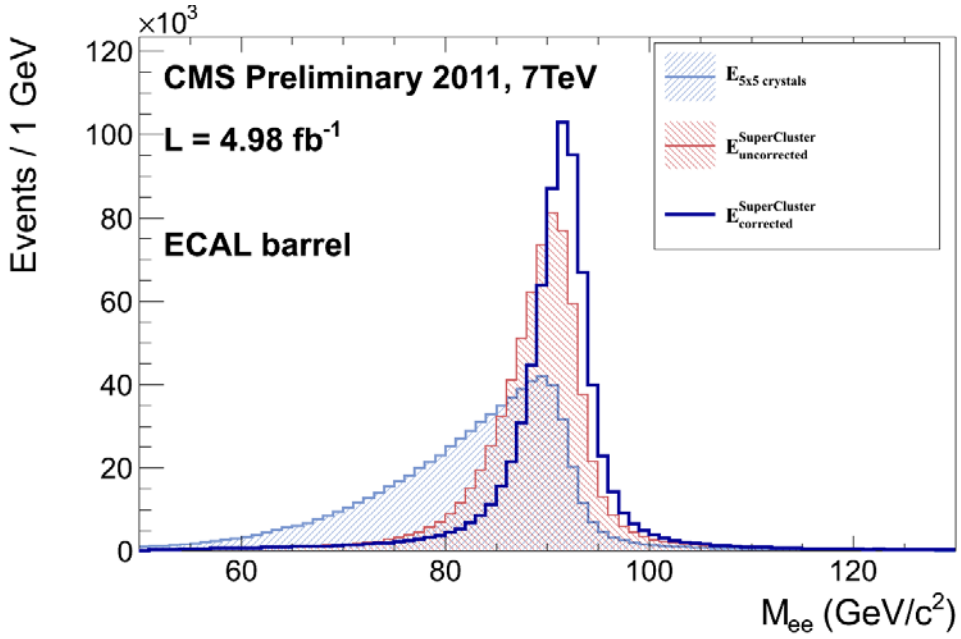

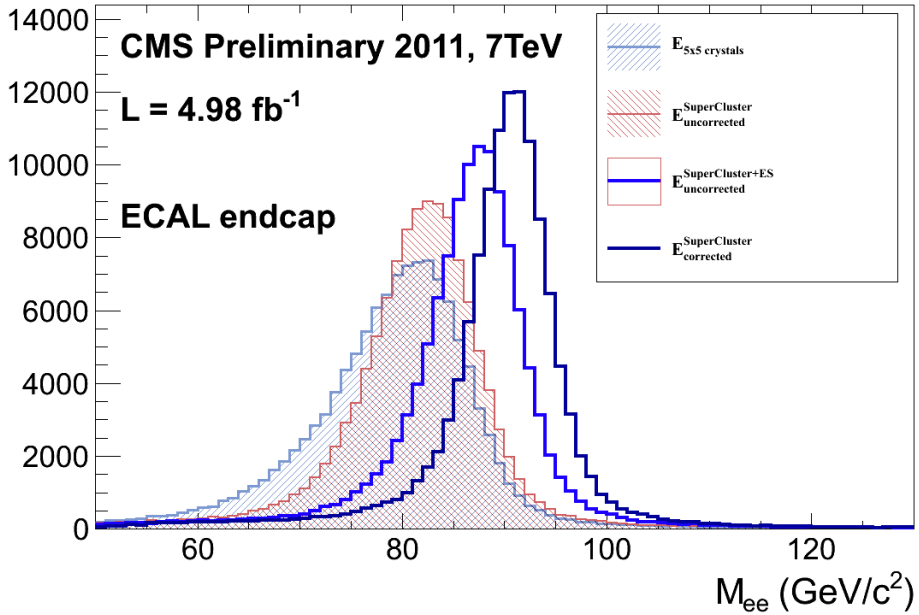

Z electrons energy resolution

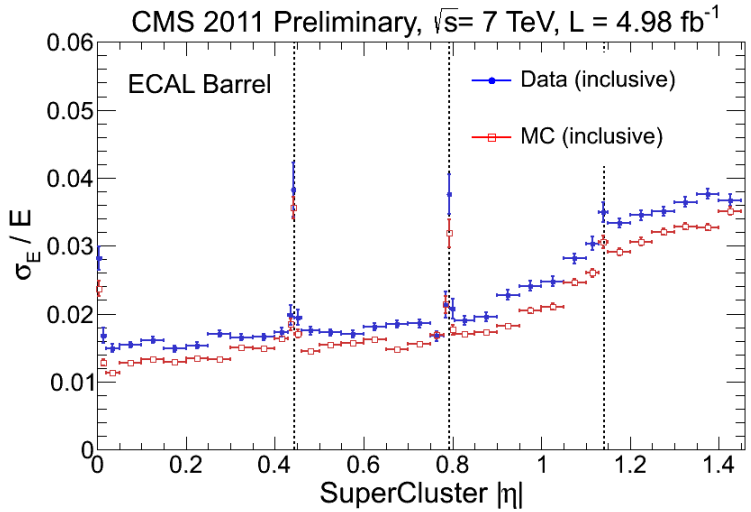

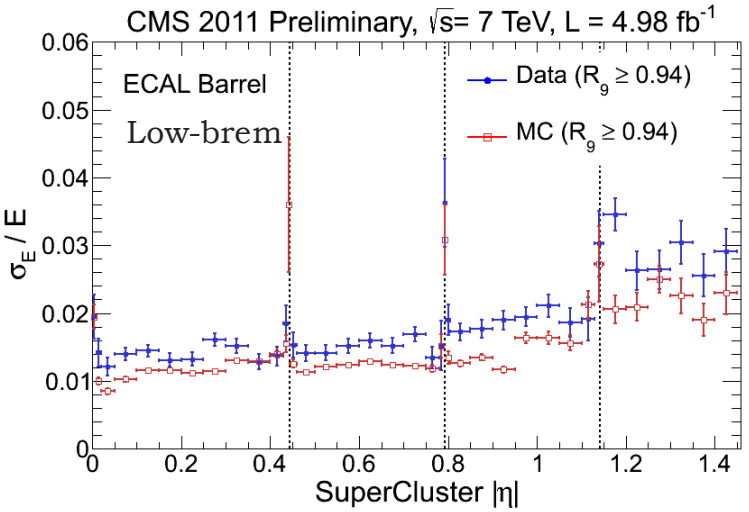

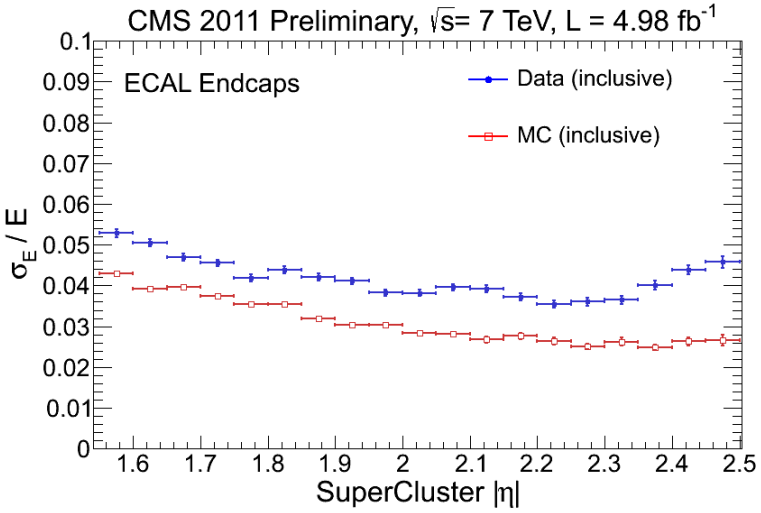

Double effort continuously ongoing to:

1. Improve the energy resolution both in Data and MC: inter-calibration precision, optimization of cluster corrections.
2. Reduce/nullify the difference between data and MC due to contributions possibly not fully simulated (improvement observed in laser correction stability, tuning of the material simulation, etc).

Alignment (in time and space)

- Timing fundamental in exotic long lived particle searches and in anomalous signal rejection.
- Time difference between the seed crystals for the two Z electrons.
- The time resolution for a single ECAL crystal, for the energy range of electrons from Z decays, is 0.19/0.28 ns in EB/EE.

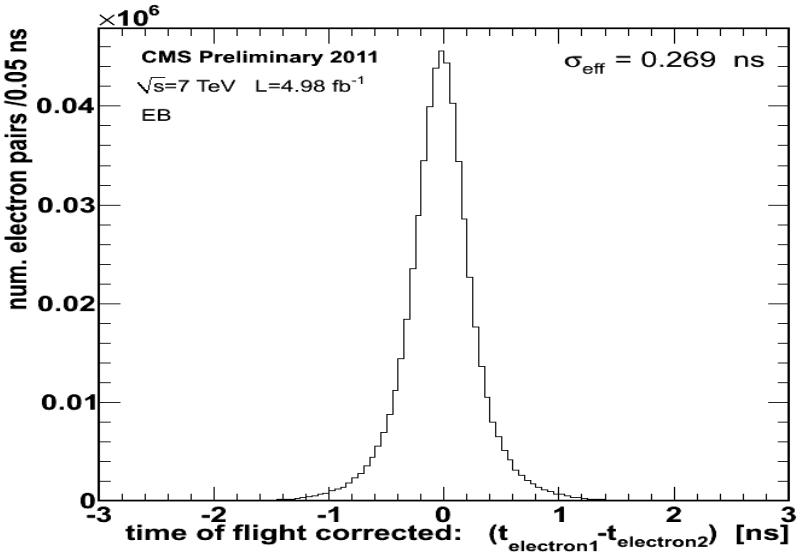

- No longitudinal segmentation of ECAL → Photon direction from shower position and identification of the interaction vertex
- Relative alignment of the ECAL crystals and the CMS tracker measured using electrons from Z→ee and W→eν events.
- Position resolution ≤ 1 mm

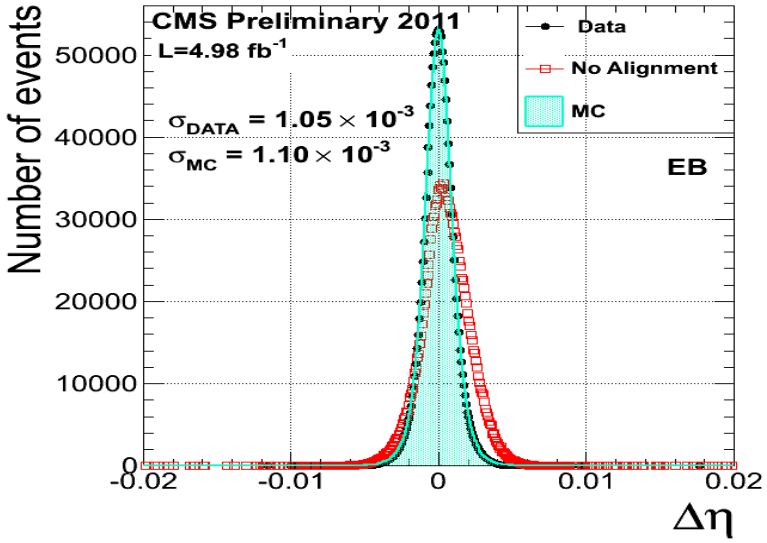

Calorimeters and discoveries: a long relationship (for instance J/Ψ, W & Z)

Final states with electrons, photons and jets also fundamental in new physics.

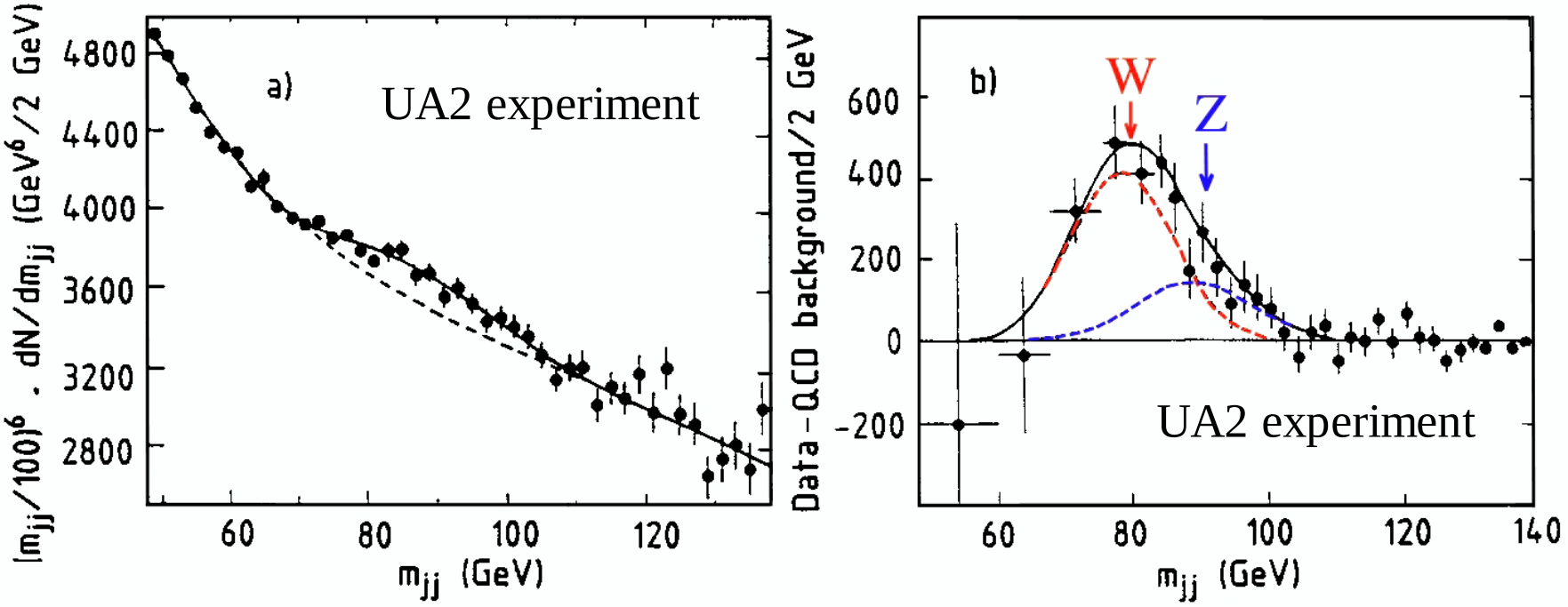

2013 NOBEL PRIZE IN PHYSICS

François Englert

Peter W. Higgs

© The Nobel Foundation. Photo: Lovisa Engblom

Calorimeters and discoveries: a long relationship

Plot from the CMS 4th July 2012 Higgs search presentation